CHAPTER 3

RING-OPENING POLYMERISATIONS : EFFECTS OF REACTION CONDITIONS AND MONOMER STRUCTURE

In this opening section of the work on the ring-opening polymerisations of the cyclic ester monomers, their polymerisabilities were studied and compared under various reaction conditions. All of the monomers previously listed on page 36 were studied except:

(a) β-propiolactone, β-butyrolactone, and pivalolactone
- commercially available but prohibitively expensive
- only purchased in small amounts sufficient for FT-IR / FT-Raman spectroscopic analysis for ring strain studies (see Chapter 5)

(b) α-methyl-β-propiolactone
- commercially unavailable
- difficult synthesis with low yield, again sufficient only for spectroscopic analysis for ring strain studies (see Chapter 5)

For the remaining 6 monomers, their polymerisabilities were studied under the following reaction conditions:

(1) in bulk (pure monomer + initiator only)

(2) at different temperatures for different times

(3) using different initiators (anionic, cationic, monomer insertion) at a 0.1 mol % initiator concentration ([Monomer] : [Initiator] = 1000 : 1 mole ratio)

The 6 monomers can be divided into 2 series:

Series I : showing the effect of ***ring size*** in lactones

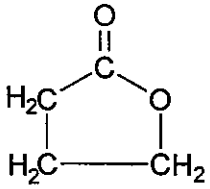

γ-butyrolactone

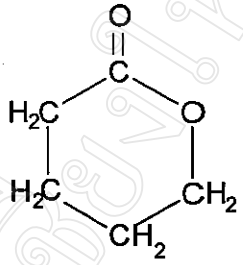

δ-valerolactone

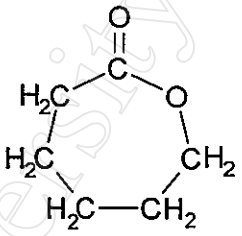

ε-caprolactone

Series II : showing the effect of ***ring substitution*** in glycolides

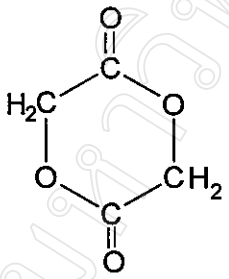

glycolide

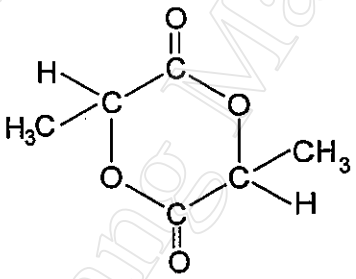

L-lactide

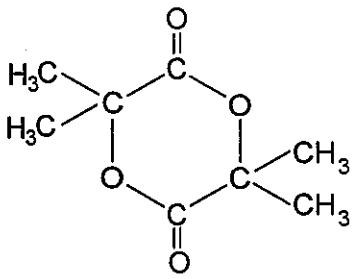

tetramethyl glycolide

The results obtained for each monomer are now described together with details of their respective polymer characterisations. In the following tables and figures:

$$\%\ \text{conversion} = \frac{\text{final weight of } \textit{purified} \text{ solid polymer}}{\text{initial weight of monomer}} \times 100$$

3.1 γ-Butyrolactone

3.1.1 Polymerisation Procedure

Despite the fact that the 5-membered ring γ-butyrolactone is generally regarded as being stable towards polymerisation, except under extreme conditions of very high pressure [61], it was included in this study as a reference monomer with which the other more reactive monomers could be compared under the same reaction conditions. The bulk polymerisations of γ-butyrolactone were carried out using the initiators, temperature and time detailed in Table 3.1. The initiators (0.1 mol %) chosen for this study were :

Name of Initiator	Abbreviation	Type
Stannous octoate*	$Sn(Oct)_2$	Monomer insertion
Boron trifluoride diethyl etherate	$BF_3 \cdot Et_2O$	Cationic
Lithium *t*-butoxide	Li(*t*-OBu)	Anionic

* systematic name : Tin(ii) bis(2-ethyl hexanoate)

Each of these 3 initiators is well known to be effective, albeit to varying extents, in the ring-opening bulk polymerisation of cyclic esters. The reaction temperature and time chosen (100°C for 96 hours) are fairly typical for ensuring that such reactions, if indeed they occur, proceed to completion. The polymerisation procedure was as follows.

γ-Butyrolactone was accurately weighed into a 7 ml screw-cap bottle with a magnetic stirrer in a dry nitrogen atmosphere glove box at room temperature. 0.1 mol % of initiator was then added and the bottle tightly sealed. The bottle was removed from the glove box and immersed in a silicone oil bath with stirring (see Fig. 3.1) at 100°C for 96 hours. At the end of the polymerisation period, the bottle was allowed to cool to room temperature. The polymerisate was then dissolved in chloroform as solvent and the polymer (if any) precipitated from solution by dropwise addition with efficient stirring into ice-cooled absolute ethanol, an appropriate non-solvent, as shown in Fig. 3.2.

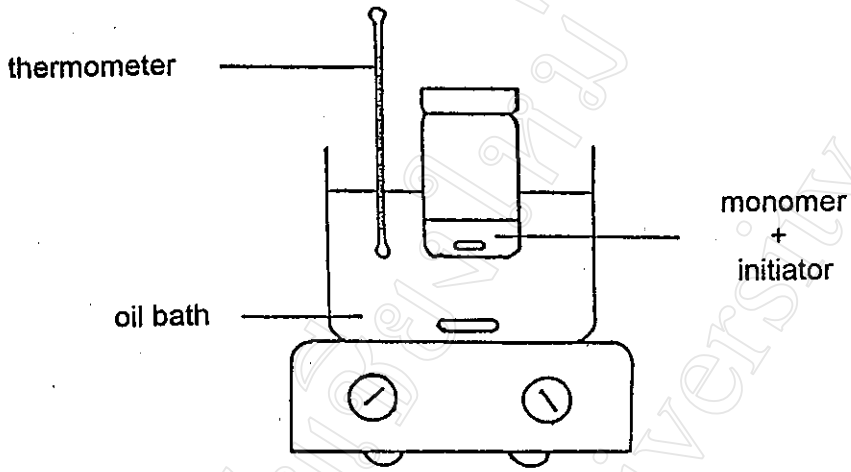

Fig. 3.1 : Apparatus used for ring-opening polymerisation.

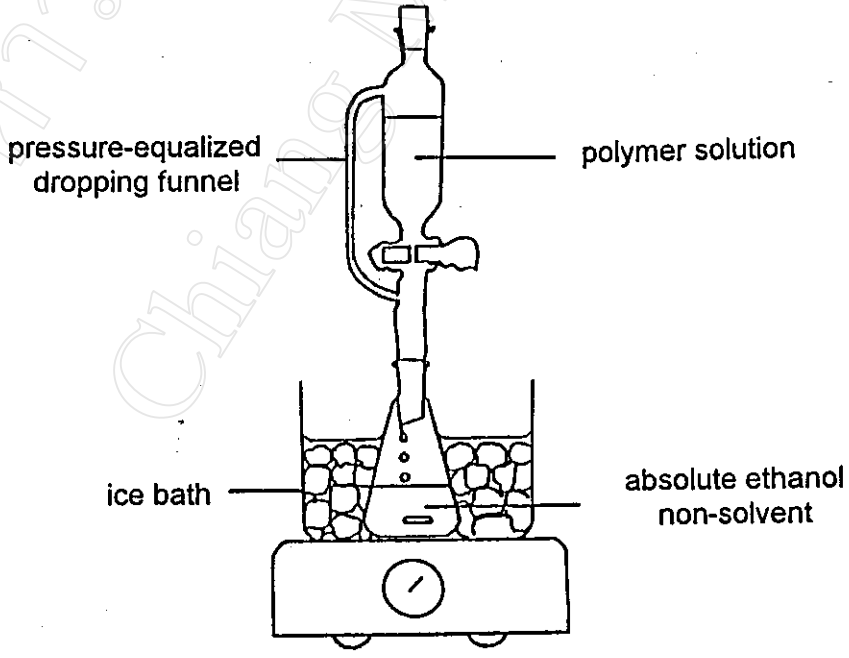

Fig. 3.2 : Apparatus used for the purification of the crude polymer by precipitation from solution.

3.1.2 Results and Conclusions

In each of the 3 polymerisations carried out, the only visibly discernable change which occurred during the timescale of the experiment was an increasing brown discoloration of the monomer. No discernable viscosity increase was observed and no solid polymer was obtained. Regarding initiator solubility in the monomer, whereas the BF_3•Et_2O appeared to be immediately soluble at the polymerisation temperature, both the $Sn(Oct)_2$ and Li(*t*-OBu) took some time to dissolve completely. However, this dissolution time was relatively short (< 1 hour) and was therefore not considered to be a rate-determining factor.

Table 3.1 : Conditions used in the polymerisation of γ-butyrolactone and details of the products obtained.

Monomer	Initiator		Temp.	Time	Physical Appearance of	Conversion
(g)	Type	Weight (g)	(°C)	(hrs.)	Final Product	(%)
3.843	$Sn(Oct)_2$	0.0184	100	96	brown liquid	0
2.718	BF_3•Et_2O	0.005	100	96	brown liquid	0
2.162	Li(*t*-OBu)	0.0021	100	96	brown liquid	0

These results in Table 3.1 are therefore consistent with expectation. γ-Butyrolactone, with its minimal ring strain, is clearly thermodynamically very stable towards ring-opening polymerisation under normal conditions. This appears to be due more to monomer stability than polymer instability. Indeed, as mentioned previously, γ-butyrolactone can be polymerised under extreme conditions yielding a polymer which is reportedly stable *".....at moderate temperatures"* (unspecified) [61]. Furthermore, the same polymer, of low molecular weight, can be synthesized via polycondensation of 4-hydroxybutyric acid ($HO\text{-}CH_2CH_2CH_2\text{-}COOH$), the parent γ-hydroxy acid. However, polymer stability / instability notwithstanding, the important conclusion as far as this work is concerned is that the 5-membered ring γ-butyrolactone has, as ring strain theory predicts, negligible tendency to polymerise. This theme will be returned to later in this thesis (Chapter 5).

3.2 δ-Valerolactone

3.2.1 Polymerisation Procedure

Unlike the 5-membered ring γ-butyrolactone, the 6-membered ring δ-valerolactone is known to polymerise quite readily under normal conditions. This is generally understood to be a reflection of the increase in ring strain as ring size increases above 5.

For δ-valerolactone, the series of polymerisation experiments that were carried out in this work are summarized in Table 3.2. The polymerisation procedure was exactly the same as that described in the previous section 3.1.1 (page 117) for γ-butyrolactone except that, in addition:

(a) a higher temperature of 150°C was also studied

(b) additional samples (each in separate bottles) were also taken at time intervals throughout the 96 hours duration of each experiment

3.2.2 Polymerisation Results

From the results in Tables 3.3-3.8 and the corresponding conversion-time profiles in Fig. 3.3, it appears that, on a purely kinetic basis, initiator efficiency is in the order of :

Initiator :	Li(*t*-OBu)	<	$Sn(Oct)_2$	<	$BF_3{\cdot}Et_2O$
Type :	anionic		monomer insertion		cationic

This is more clearly evident at the lower polymerisation temperature of 100°C in Fig. 3.3(a) and supports the view that the δ-valerolactone ring is more susceptible to cationic than anionic attack. In this context, it is worth noting here that, in the case of the monomer insertion mechanism, the actual ring-opening step, although generally referred to as being non-ionic in nature, probably does have a semblance of cationic character by virtue of the alternative Lewis acid hydrolysis mechanism. These mechanisms will be discussed in detail in Chapter 6.

It is also worth noting in Fig. 3.3 that each polymerisation proceeds to high conversion (> 75%) with the maximum value being attained within the first 48 hours; the Li(*t*-OBu)-initiated reaction at 100°C is the sole exception. Again, initiator solubility did not appear to be an influential factor. The $BF_3{\cdot}Et_2O$ initiator was instantly soluble in the δ-valerolactone monomer, while the $Sn(Oct)_2$ and Li(*t*-OBu) initiators dissolved completely within the first hour of the reaction. As would be expected, the reaction rate increased at the higher temperature but the maximum % conversion decreased slightly. This latter observation is undoubtedly due to the onset of depolymerisation as the polymer's thermal decomposition temperature is approached. This is particularly evident in Fig. 3.3(b) for $Sn(Oct)_2$ at 150°C which shows a slowly but consistently decreasing % conversion with time after the maximum has been attained. $Sn(Oct)_2$ is known to be an effective transesterification catalyst which, in the case of poly(δ-valerolactone), (PVL), would facilitate the intramolecular ester interchange mechanism leading to monomer elimination. It must therefore be concluded from these results that the higher temperature of 150°C is, in fact, slightly too high for δ-valerolactone polymerisation.

Table 3.2 : Summary of δ-valerolactone polymerisation experiments.

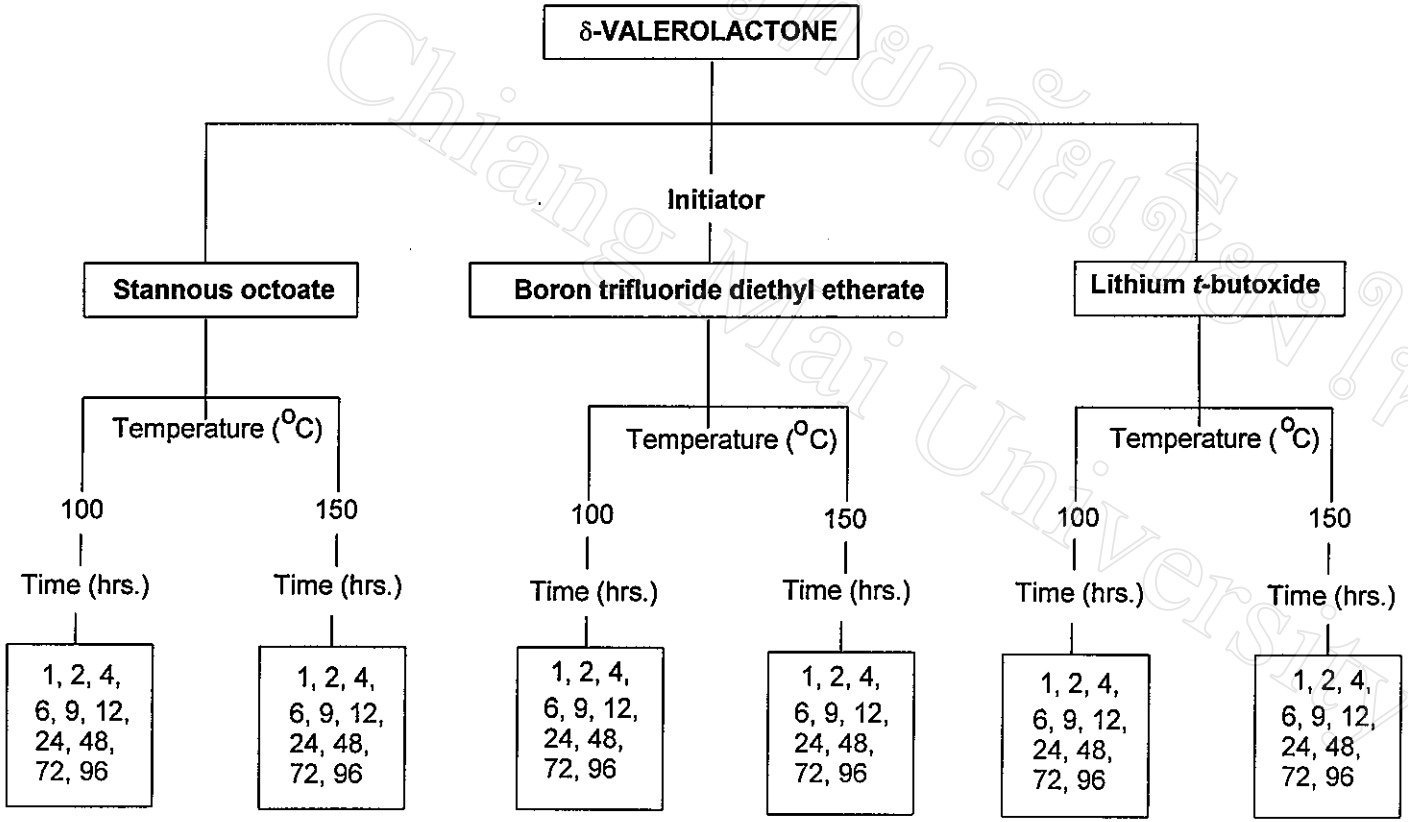

Table 3.3 : Polymerisations of δ-valerolactone at 100°C using stannous octoate as initiator.

Monomer (g)	Initiator (g)	Time (hrs.)	Physical Appearance of Product at Room Temp.		Conversion (%)
			Crude	Purified	
1.005	0.0042	1	colourless liquid	no solid ppte.	0
1.000	0.0038	2	colourless liquid	no solid ppte.	0
1.002	0.0042	4	waxy solid	no solid ppte.	0
1.006	0.0039	6	waxy solid	no solid ppte.	0
1.004	0.0042	9	waxy solid	no solid ppte.	0
1.016	0.0042	12	white solid	white powder	44.7
1.033	0.0039	24	white solid	white powder	79.9
1.010	0.0042	48	white solid	white powder	90.2
1.006	0.0040	72	white solid	white powder	88.9
1.004	0.0041	96	white solid	white powder	89.1

Table 3.4 : Polymerisations of δ-valerolactone at 150°C using stannous octoate as initiator.

Monomer (g)	Initiator (g)	Time (hrs.)	Physical Appearance of Product at Room Temp.		Conversion (%)
			Crude	Purified	
1.003	0.0040	1	white solid	white powder	61.3
1.018	0.0040	2	white solid	white powder	64.6
0.997	0.0041	4	white solid	white powder	61.1
1.004	0.0040	6	white solid	white powder	82.5
1.011	0.0041	9	white solid	white powder	86.6
1.004	0.0040	12	white solid	white powder	74.2
1.007	0.0041	24	white solid	white powder	83.3
1.003	0.0040	48	white solid	white powder	80.0
1.006	0.0040	72	white solid	white powder	79.5
0.998	0.0040	96	white solid	white powder	76.2

Table 3.5 : Polymerisations of δ-valerolactone at 100°C using boron trifluoride diethyl etherate as initiator.

Monomer (g)	Initiator (g)	Time (hrs.)	Physical Appearance of Product at Room Temp.		Conversion (%)
			Crude	Purified	
2.633	0.005	1	brown solid	brown powder	48.5
3.069	0.006	2	brown solid	brown powder	60.9
2.121	0.004	4	brown solid	brown powder	71.4
2.005	0.004	6	brown solid	brown powder	77.0
2.110	0.004	9	brown solid	brown powder	88.7
2.121	0.004	12	brown solid	brown powder	93.2
2.653	0.005	24	brown solid	brown powder	90.2
2.119	0.004	48	brown solid	brown powder	96.2
2.110	0.004	72	brown solid	brown powder	92.3
2.127	0.004	96	brown solid	brown powder	94.5

Table 3.6 : Polymerisations of δ-valerolactone at 150°C using boron trifluoride diethyl etherate as initiator.

Monomer (g)	Initiator (g)	Time (hrs.)	Physical Appearance of Product at Room Temp.		Conversion (%)
			Crude	Purified	
2.118	0.004	1	brown solid	brown powder	77.5
2.134	0.004	2	brown solid	brown powder	80.0
2.657	0.005	4	brown solid	brown powder	87.8
2.116	0.004	6	brown solid	brown powder	88.7
2.651	0.005	9	brown solid	brown powder	80.1
2.130	0.004	12	brown solid	brown powder	88.5
3.181	0.006	24	brown solid	brown powder	82.4
2.641	0.005	48	brown solid	brown powder	90.9
2.121	0.004	72	brown solid	brown powder	86.2
2.643	0.005	96	brown solid	brown powder	85.8

Table 3.7 : Polymerisations of δ-valerolactone at 100°C using lithium *t*-butoxide as initator.

Monomer (g)	Initiator (g)	Time (hrs.)	Physical Appearance of Product at Room Temp.		Conversion (%)
			Crude	Purified	
2.505	0.0021	1	brown solution	no solid ppte.	0
2.513	0.0020	2	brown solution	no solid ppte.	0
2.512	0.0019	4	brown solution	no solid ppte.	0
.2.504	0.0020	6	brown solution	no solid ppte.	0
2.503	0.0021	9	brown solution	no solid ppte.	0
2.498	0.0020	12	brown solution	no solid ppte.	0
2.509	0.0020	24	brown solid	fawn powder	14.2
2.587	0.0020	48	brown solid	fawn powder	31.1
2.499	0.0020	72	brown solid	fawn powder	73.1
2.505	0.0019	96	brown solid	fawn powder	77.9

Table 3.8 : Polymerisations of δ-valerolactone at 150°C using lithium *t*-butoxide as initator.

Monomer (g)	Initiator (g)	Time (hrs.)	Physical Appearance of Product at Room Temp.		Conversion (%)
			Crude	Purified	
2.502	0.0020	1	brown solution	no solid ppte.	0
2.499	0.0021	2	brown solution	no solid ppte.	0
2.501	0.0020	4	brown solution	fawn powder	24.0
2.509	0.0020	6	brown solution	fawn powder	32.8
2.509	0.0020	9	brown solid	fawn powder	44.1
2.510	0.0021	12	brown solid	fawn powder	63.2
2.516	0.0021	24	brown solid	fawn powder	81.9
2.506	0.0019	48	brown solid	fawn powder	80.0
2.513	0.0019	72	brown solid	fawn powder	80.0
2.498	0.0020	96	brown solid	fawn powder	82.6

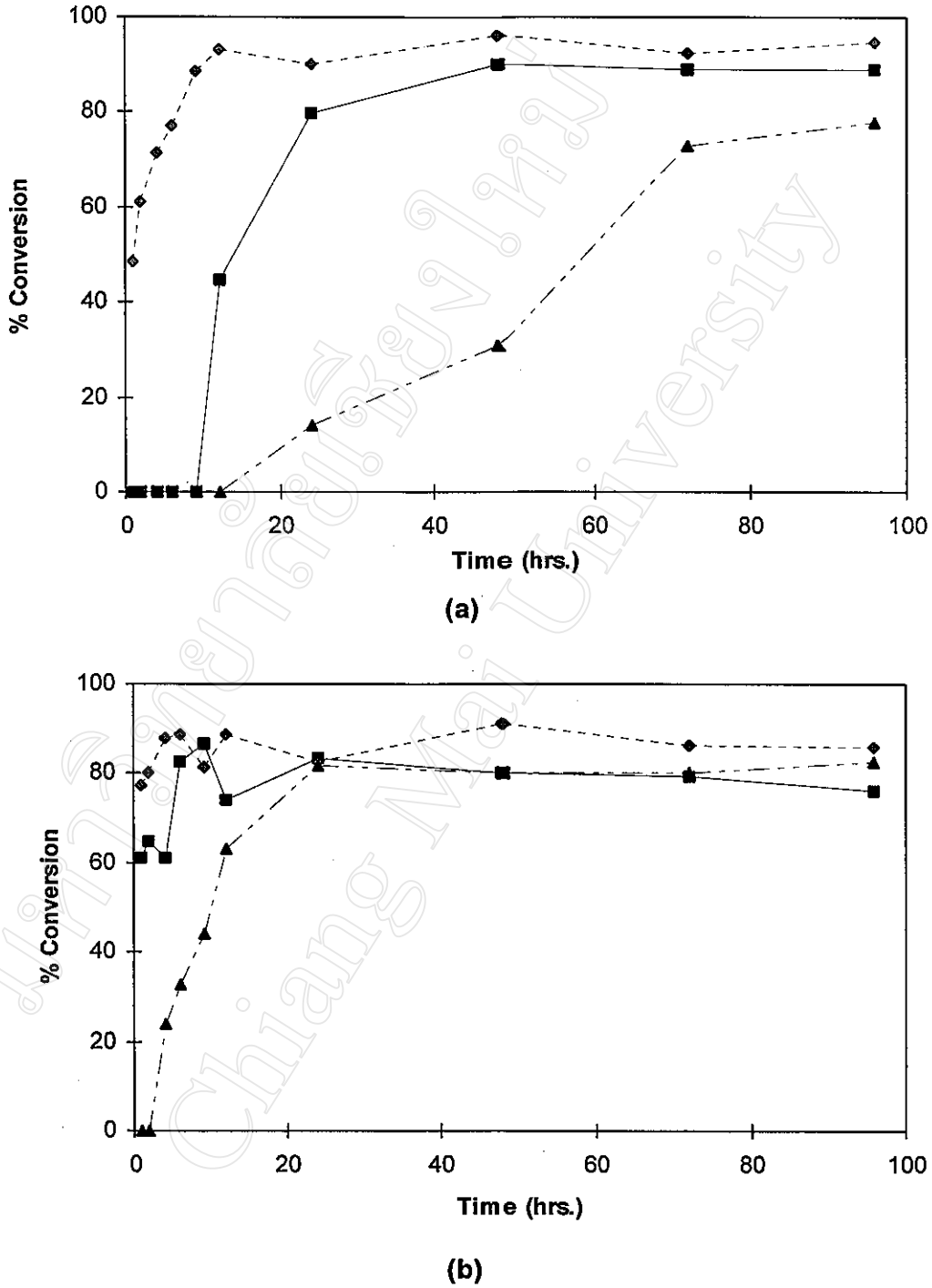

Fig. 3.3 : Comparison of δ-valerolactone conversion-time profiles using different initiators at (a) 100°C and (b) 150°C.

3.2.3 Polymer Characterisation

3.2.3.1 Chemical Structure

A typical infrared spectrum of one of the purified poly(δ-valerolactone) (PVL) products is shown in Fig. 3.4. The spectrum, which was obtained from a sample prepared in the form of a thin film cast from solution in chloroform, compares very closely with the reference spectrum in Fig. 3.5. The major vibrational peak assignments are listed in Table 3.9.

Table 3.9 : Infrared absorption band assignments for poly(δ-valerolactone).

Vibrational Assignment	Band Intensity*	Wavenumber (cm^{-1})
O-H stretching, in OH / COOH end-groups	w	3600-3400
C-H stretching, in CH_2	m	2961, 2911
C=O stretching	s	1723
C-H bending, in CH_2	m	1421-1400
C-O stretching, acyl-oxygen	m	1253
C-O stretching, alkyl-oxygen	m	1060

* w = weak m = medium s = strong

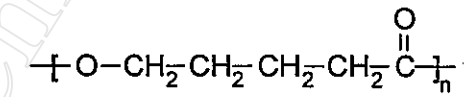

poly(δ-valerolactone), PVL

The PVL spectrum in Fig 3.4 is therefore seen to be consistent with the polymer's chemical structure. It is also worth noting that the O-H stretching peak in the region of 3400-3600 cm^{-1}, due to the presence of residual OH and/or COOH end-groups in the polymer, is extremely small for this particular sample. This is indicative of at least a reasonable level of molecular weight attainment, an indication confirmed by GPC analysis ($\overline{M}_n$ = 10650, $\overline{DP}_n$ = 106) as described later in section 3.2.3.4.

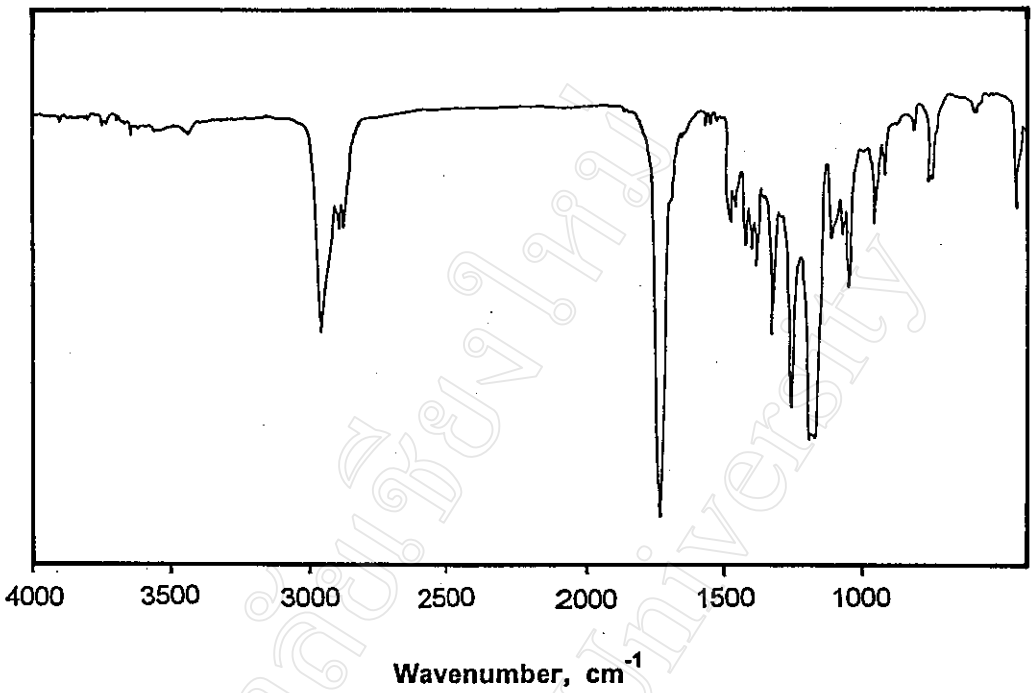

Fig. 3.4 : Infrared spectrum of purified poly(δ-valerolactone) synthesized at 150°C for 24 hours using stannous octoate as initiator.

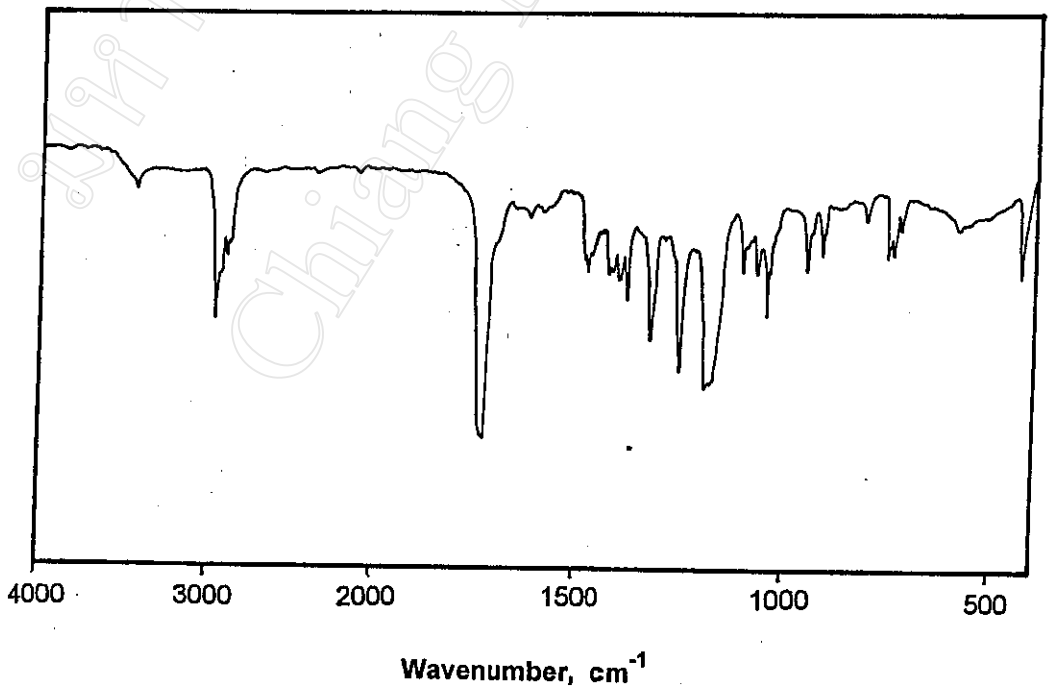

Fig 3.5 : Reference infrared spectrum of poly(δ-valerolactone) [82].

3.2.3.2 Temperature Transitions

As mentioned previously in section 2.3.5, the temperature transitions in a polymer are most conveniently characterised by differential scanning calorimetry (DSC). A typical DSC curve for the purified PVL samples prepared in this work is illustrated in Fig. 3.6 showing the crystalline melting endotherm. The heat of melting (ΔH_m = 94.24 J/g) printed out on Fig. 3.6 is a measure of the polymer's % crystallinity. The actual value of the % crystallinity cannot be calculated from the equation below, however, because the theoretical heat of melting for a 100% crystalline sample (ΔH_m^*) is not available in the reference literature (e.g., the *"Polymer Handbook"* [84]) for PVL.

$$\% \text{ crystallinity} = \frac{\Delta H_m}{\Delta H_m^*} \times 100\ \%$$

Also in Fig 3.6, the polymer's melting peak temperature of 57.71°C, which is usually taken as its melting point, T_m (corrected to 58°C), is in close agreement with literature values for PVL (e.g., T_m = 53-55°C [84]). Such low T_m values (< 100°C) are characteristic of many aliphatic polyesters. Apart from the melting transition, no other temperature transitions are evident in Fig. 3.6. The polymer's glass transition temperature, T_g, is sub-ambient and could not be measured by the DSC instrument set-up available in this work.

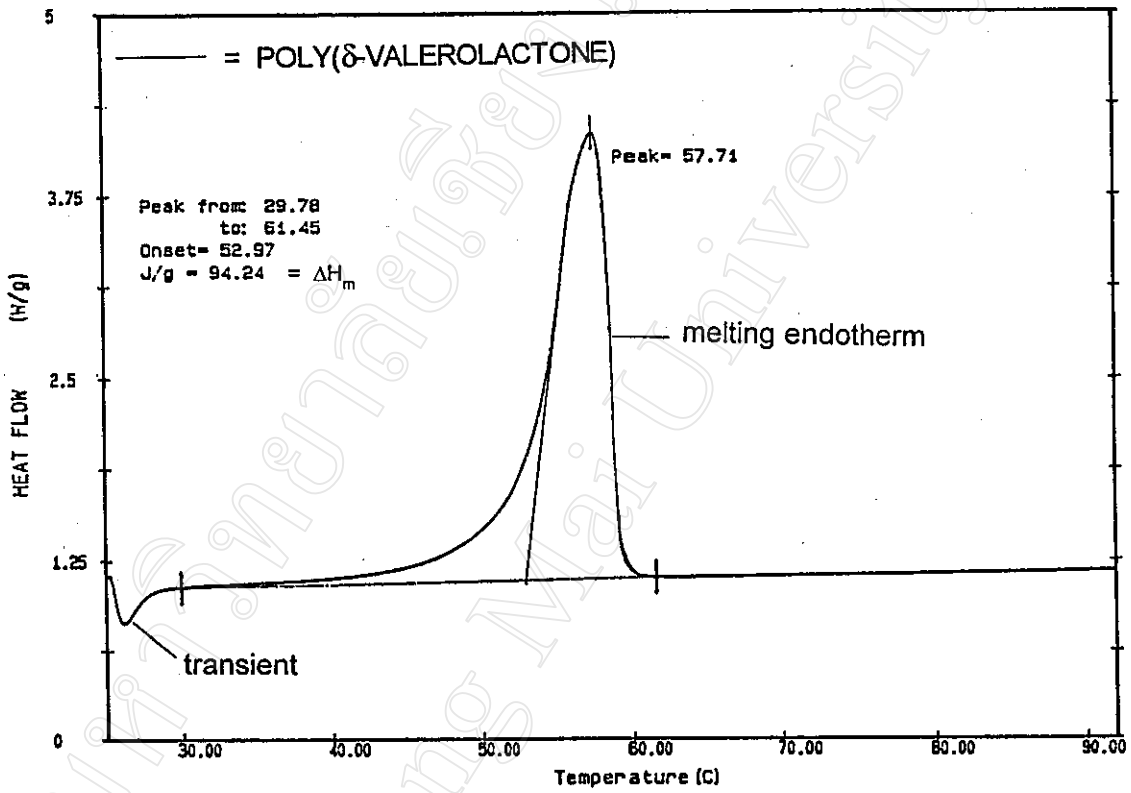

Fig. 3.6 : DSC thermogram of purified poly(δ-valerolactone) synthesized at 150°C for 24 hours using stannous octoate as initiator.

(Heating rate = 10°C/min; atmosphere = dry N_2)

3.2.3.3 Thermal Stability

Polymer thermal stability over a range of temperature is conveniently studied by non-isothermal thermogravimetry (TG). A typical TG curve for the PVL synthesized here is shown in Fig. 3.7. The curve shows an essentially complete (>99%) single-step weight loss over the temperature range 190-390°C.

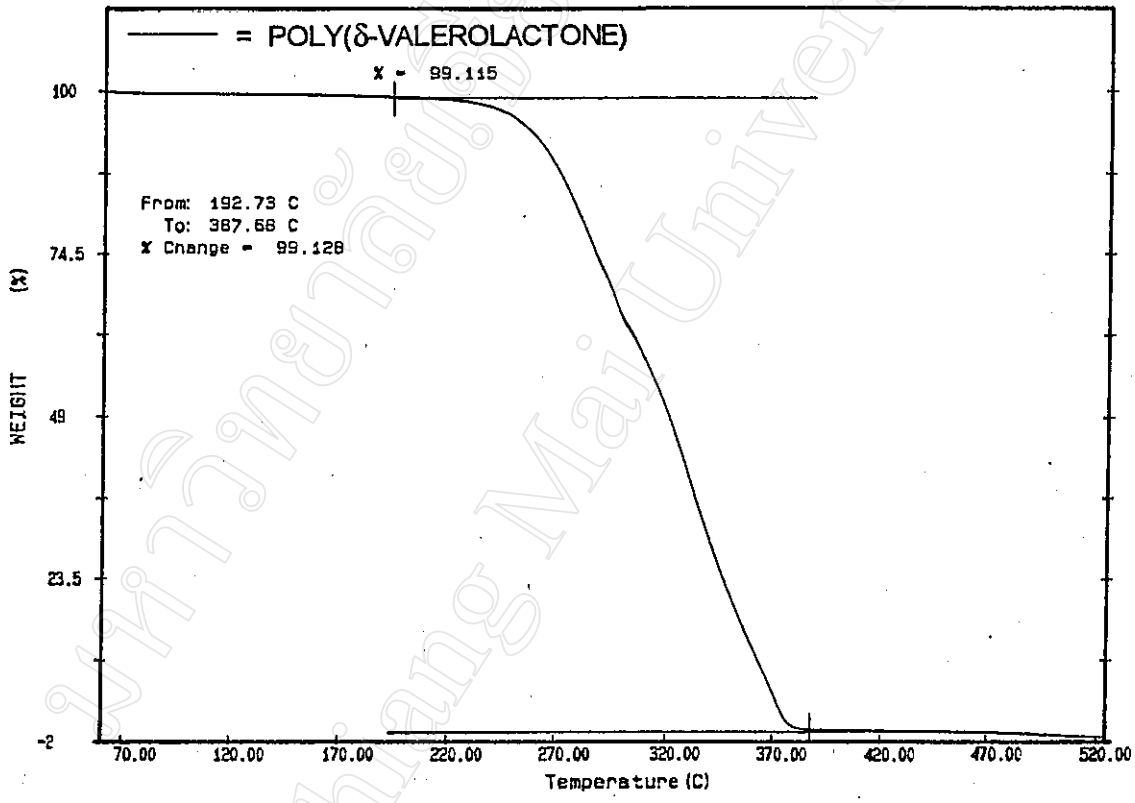

Fig. 3.7 : TG thermogram of purified poly(δ-valerolactone) synthesized at 150°C for 24 hours using stannous octoate as initiator.

(Heating rate = 20°C/min; atmosphere = dry N_2)

This thermal decomposition range has important implications for the polymer's synthesis, especially in cyclic ester polymerisation where a ring-chain equilibrium exists around a ***"ceiling temperature"***. In this particular example of PVL, the initial decomposition (weight loss) temperature of around 190°C is not far removed from the higher of the two synthesis temperatures of 150°C. Indeed, this temperature difference is probably even less when it is considered that bond scission at the molecular level undoubtedly precedes product volatilisation. Consequently, the thermal stability of the polymer as it is formed at the polymerisation temperature, and this seems to be particularly relevant to PVL, can have a major influence on the progress of the polymerisation reaction. This will be discussed further in the light of the molecular weight results in the following section.

3.2.3.4 Molecular Weight

In this study, the main method of molecular weight determination was gel permeation chromatography (GPC). As described previously in section 2.3.8, GPC measurements were performed in tetrahydrofuran (THF) as solvent at 30°C in a column calibrated by narrow molecular weight distribution polystyrene standards. Typical GPC curves and their related data print-out for a PVL sample are shown in Fig. 3.8.

Since the build-up of molecular weight during a polymerisation reaction provides valuable information about the nature of the reaction itself, the molecular weights of all the PVL samples prepared in this study were subjected to GPC analysis. The results are summarized in Tables 3.10-3.15 for each of the 3 initiators used at each of the 2 polymerisation temperatures. The values of the various molecular weight averages given in the Tables are taken directly from the GPC data print-outs without any attempt to correct them to the appropriate number of significant figures. As a rough estimate, the range of uncertainty in the various $\bar{M}$ values is probably within about ± 5%.

For ease of comparison, the $\bar{M}_n$-time profiles are plotted in Fig. 3.9. From these graphs, the following general comments can be made:

(1) Characteristic of ring-opening polymerisation, and mechanistically similar to addition polymerisation, the polymer molecular weights increase rapidly from the start of the reaction up to fairly constant levels.

(2) Apart from isolated data points, most notably in the $Sn(Oct)_2$ profiles, there does not appear to be a great deal of difference in the profiles for the 3 initiators, at least not enough to draw firm conclusions. Perhaps the only clear difference lies in the Li(*t*-OBu) profiles which do seem to indicate a slower build-up in molecular weight compared with the other 2 initiators, similar to their conversion-time profiles previously.

(3) Comparing Fig. 3.9 (a) and (b), the results do not show any significant decrease in molecular weight at the higher temperature of 150°C, despite the earlier indications of thermal decomposition. This suggests that thermal decomposition, if indeed it occurs, is more likely to proceed via intramolecular ester interchange, eliminating monomer units as shown below, rather than via random chain scission.

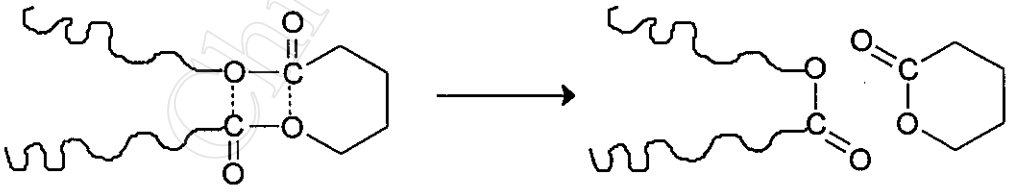

(4) The polydispersity indices, $\overline{M}_w / \overline{M}_n$, in Tables 3.10-3.15 show no obvious trends except that those for the Li(*t*-OBu)-initiated samples are slightly less than the others, indicating narrower molecular weight distributions.

TECHNICAL SERVICE, NATIONAL METAL AND MATERIALS TECHNOLOGY CENTER

Version 3.00a - MULTIDETECTOR GPC SOFTWARE - revised 03/17/93 J.Lesec

PVL/0.1%Sn(Oct)2/@150C/24hrs RESULTS Fri 29 AUG 1997 16:28:52
Polystyrene - 3 # 1 RUN # 13 Inj # 12 CODE : INJ 151
DATE : Thu 28 AUG 1997 TIME : 13:08:47 Manual integration
Calibration # 1.003 Number of points: 219 Axial dispersion: NO

MOLECULAR WEIGHTS UNIVERSAL

Peak mol. wt Mp :	19020	
Number aver. Mn :	10650	
Viscos. aver. Mv :	18640	
Weight averag.Mw :	20520	
Z average Mz :	32130	
Polydispersity :	1.93	
[n] (ml/g) :	34.12	
Log(K) (M-H) :	-1.184	
Alpha (M-H) :	.636	

REFRACTOMETER C/c : 1	Peak elution : 16.38	Baseline : .099203
Area constant : 2.126	Conc. (g/ml) : .00466	dn/dc : 0
VISCOMETER Mn : 12990	Peak elution : 16.054	Baseline : .89
[n]area (ml/g): 33.53	[n]peak(ml/g): 43.53	[n]exp (ml/g): 34.12

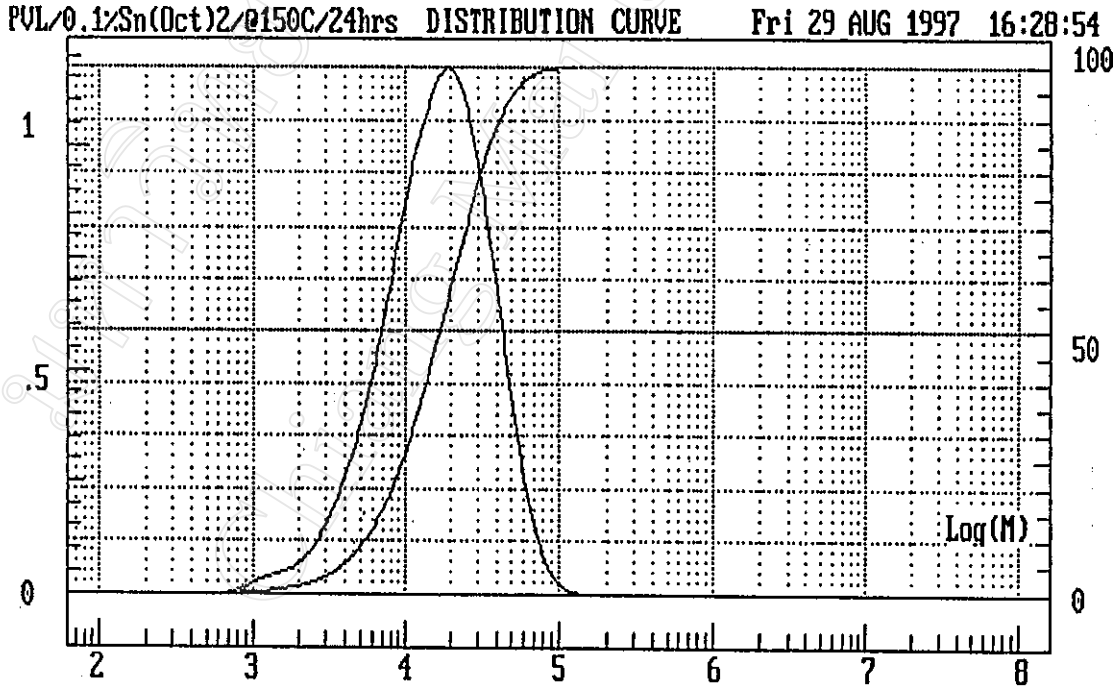

Fig. 3.8 : GPC curves and data print-out for purified poly(δ-valerolactone) synthesized at 150°C for 24 hours using stannous octoate as initiator.

Table 3.10 : GPC molecular weight averages and polydispersity indices for the PVL synthesized at 100°C using stannous octoate as initiator.

Polymerisation Time (hrs.)	Molecular Weight Averages			$\bar{M}_w / \bar{M}_n$
	$\bar{M}_n$	$\bar{M}_v$	$\bar{M}_w$	
12	3873	5033	5493	1.42
24	6519	9970	12460	1.91
48	18310	31950	35850	1.96
72	10210	15900	17550	1.72
96	8920	14170	16130	1.81

Table 3.11 : GPC molecular weight averages and polydispersity indices for the PVL synthesized at 150°C using stannous octoate as initiator.

Polymerisation Time (hrs.)	Molecular Weight Averages			$\bar{M}_w / \bar{M}_n$
	$\bar{M}_n$	$\bar{M}_v$	$\bar{M}_w$	
1	9698	19590	23050	2.38
2	20700	34180	37360	1.80
4	12490	23540	25500	2.04
6	9421	17430	18270	1.94
9	9249	17130	19580	2.12
12	8906	15540	17360	1.95
24	10650	18640	20520	1.93
48	8316	16200	19160	2.30
72	8433	15190	17300	2.05
96	16430	26180	29370	1.79

Table 3.12 : GPC molecular weight averages and polydispersity indices for the PVL synthesized at 100°C using boron trifluoride diethyl etherate as initiator.

Polymerisation Time (hrs.)	Molecular Weight Averages			$\bar{M}_w / \bar{M}_n$
	$\bar{M}_n$	$\bar{M}_v$	$\bar{M}_w$	
1	8612	14530	16630	1.93
2	9328	16780	19460	2.09
4	9636	16190	18180	1.89
6	9819	17520	20150	2.05
9	9881	16800	18730	1.90
12	9938	16750	18560	1.87
24	9384	17310	20300	2.16
48	8944	15540	18130	2.03
72	7949	13300	15370	1.93
96	9798	17020	19030	1.94

Table 3.13 : GPC molecular weight averages and polydispersity indices for the PVL synthesized at 150°C using boron trifluoride diethyl etherate as initiator.

Polymerisation Time (hrs.)	Molecular Weight Averages			$\bar{M}_w / \bar{M}_n$
	$\bar{M}_n$	$\bar{M}_v$	$\bar{M}_w$	
1	8872	14550	16670	1.88
2	10950	16540	18280	1.67
4	9092	15290	17740	1.95
6	7127	12690	15760	2.21
9	6496	11160	13680	2.11
12	6298	10260	12020	1.91
24	6374	10240	11750	1.84
48	7387	12290	13670	1.85
72	6951	11470	13300	1.91
96	8224	13230	14460	1.76

Table 3.14 : GPC molecular weight averages and polydispersity indices for the PVL synthesized at 100°C using lithium *t*-butoxide as initiator.

Polymerisation Time (hrs.)	Molecular Weight Averages			$\bar{M}_w / \bar{M}_n$
	$\bar{M}_n$	$\bar{M}_v$	$\bar{M}_w$	
24	2695	3243	3550	1.32
48	4469	5611	6199	1.39
72	6957	8131	8652	1.24
96	4574	6414	7148	1.56

Table 3.15 : GPC molecular weight averages and polydispersity indices for the PVL synthesized at 150°C using lithium *t*-butoxide as initiator.

Polymerisation Time (hrs.)	Molecular Weight Averages			$\bar{M}_w / \bar{M}_n$
	$\bar{M}_n$	$\bar{M}_v$	$\bar{M}_w$	
4	3586	4786	5846	1.63
6	3765	4895	6024	1.60
9	3865	5028	6511	1.68
12	5637	6767	7075	1.25
24	7571	11130	12730	1.68
48	8081	12270	13130	1.63
72	8083	12590	13600	1.68
96	13530	21530	23770	1.76

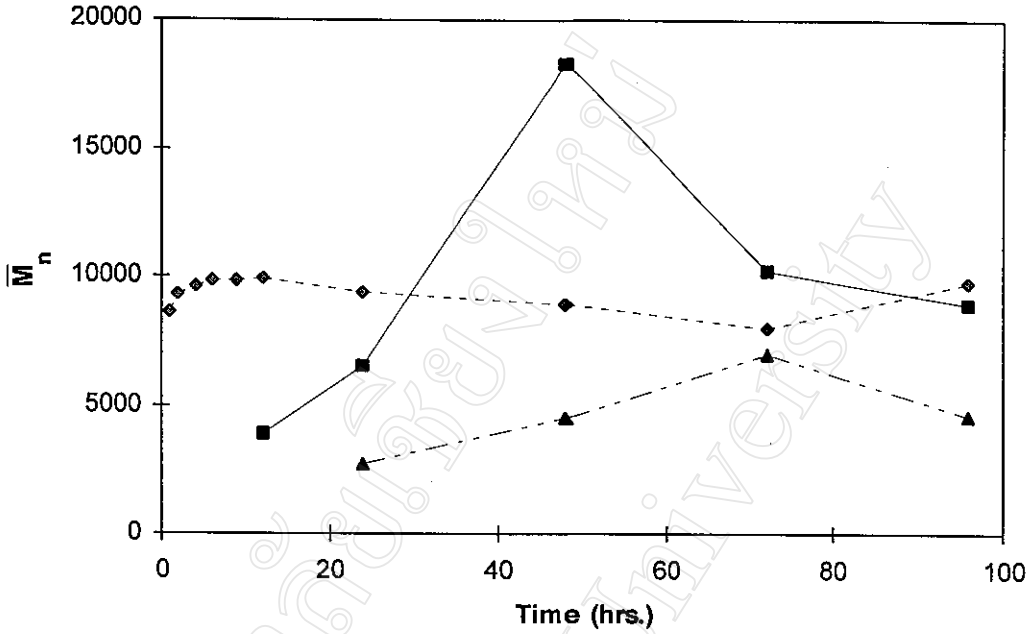

(a)

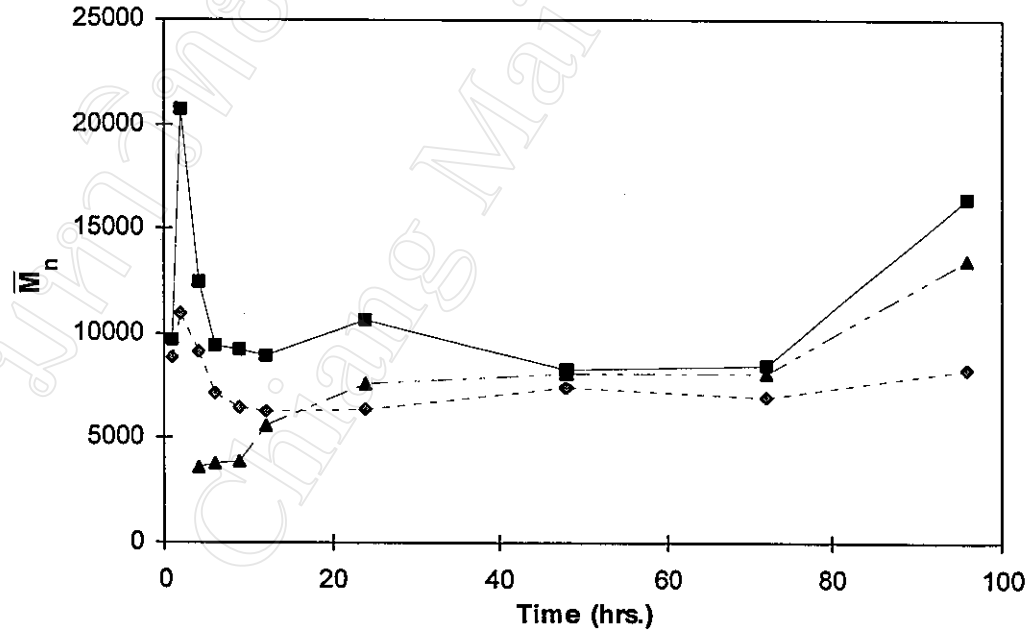

(b)

Fig. 3.9 : Comparison of PVL number-average molecular weight $\bar{M}_n$-time profiles using different initiators at (a) 100°C and (b) 150°C.

$Sn(Oct)_2$

$BF_3{\cdot}Et_2O$

Li(*t*-OBu)

3.3 ε-Caprolactone

3.3.1 Polymerisation Procedure

ε-Caprolactone, like δ-valerolactone previously, is known to polymerise quite readily under normal conditions. Indeed, its larger 7-membered ring, with its slightly greater ring strain, should further encourage the process of ring opening. Its polymer, poly(ε-caprolactone) (PCL) is well documented in the polymer literature, much more so than other polylactones. This is due, at least in part, to its relatively low cost since ε-caprolactone monomer can be produced quite cheaply from the oxidation of cyclohexanone. However, because of its low melting point (approx. 60°C), PCL has only achieved very limited commercial importance in applications which take advantage of either its biodegradability or its unusually high level of compatibility with poly(vinyl chloride).

For ε-caprolactone, the series of polymerisation experiments that were carried out in this work are summarized in Table 3.16. The polymerisation procedure employed was exactly the same as that described in the previous section 3.2.1 (page 120) for δ-valerolactone. Again, the experiments were treated as kinetic experiments with samples being taken at different time intervals.

Table 3.16 : Summary of ε-caprolactone polymerisation experiments.

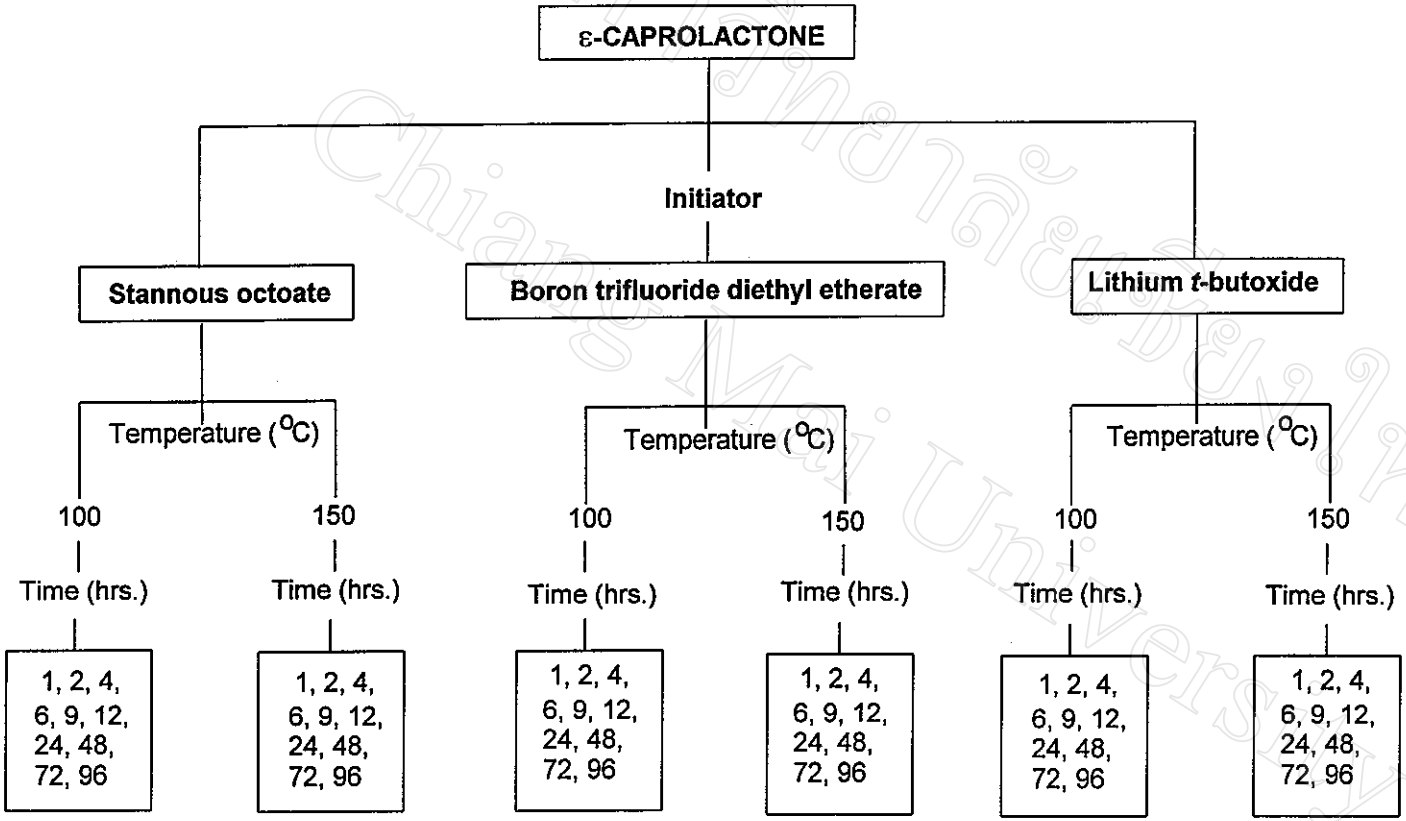

3.3.2 Polymerisation Results

From the results in the following Tables 3.17-3.22 and the corresponding kinetic profiles in Fig. 3.10, initiator efficiency is again in the order of:

Initiator	:	Li(*t*-OBu)	<	$Sn(Oct)_2$	<	$BF_3{\cdot}Et_2O$
Type	:	anionic		monomer insertion		cationic

While this order is clearly evident in Fig. 3.10(a) at the lower polymerisation temperature of 100°C, the distinction between $Sn(Oct)_2$ and $BF_3{\cdot}Et_2O$ disappears at 150°C in Fig. 3.10(b). These results seem to suggest that the different initiators, with their different mechanisms, each have their own quite specific energy requirements which govern the temperature range over which they are effective. Again, initiator solubility in the monomer did not appear to exert an important influence, although the fact that $BF_3{\cdot}Et_2O$ was instantly soluble, whereas both Li(*t*-OBu) and $Sn(Oct)_2$ took a little time (< 1 hour) to dissolve, may well have contributed to its overall effectiveness.

Despite the differences in rate, the one thing that the ε-caprolactone polymerisation experiments had in common was that, once started, the reactions proceeded to high (> 80%) conversion. Furthermore, the final conversions did not decrease at the higher temperature of 150°C, in contrast to the previous δ-valerolactone experiments. This is an indication that PCL is thermally more stable towards depolymerisation than PVL or, to put it another way, that ε-caprolactone polymerisation has a higher *ceiling temperature* than that of δ-valerolactone. This subject of thermal stability will be returned to in the following section 3.3.3.3.

Finally, as regards the physical appearances of the purified polymers, the $Sn(Oct)_2$-initiated products were the only ones which showed no brown discoloration. It is unclear exactly which structural moieties give rise to this discoloration but they seem to be related to the choice of initiator and, possibly, to the nature and thermal stability of its derivatives/complexes formed during the course of the reaction.

Table 3.17 : Polymerisations of ε-caprolactone at 100°C using stannous octoate as initiator.

Monomer (g)	Initiator (g)	Time (hrs.)	Physical Appearance of Product at Room Temp.		Conversion (%)
			Crude	Purified	
1.144	0.0040	1	colourless liquid	no solid ppte.	0
1.143	0.0042	2	colourless liquid	no solid ppte.	0
1.133	0.0039	4	colourless liquid	no solid ppte.	0
1.148	0.0040	6	colourless liquid	no solid ppte.	0
1.176	0.0041	9	waxy solid	no solid ppte.	0
1.141	0.0039	12	white solid	white powder	0.1
1.145	0.0042	24	white solid	white powder	22.1
1.166	0.0042	48	white solid	white powder	86.3
1.130	0.0040	72	white solid	white powder	85.8
1.155	0.0042	96	white solid	white powder	89.6

Table 3.18 : Polymerisations of ε-caprolactone at 150°C using stannous octoate as initiator.

Monomer (g)	Initiator (g)	Time (hrs.)	Physical Appearance of Product at Room Temp.		Conversion (%)
			Crude	Purified	
1.137	0.0039	1	white solid	white powder	77.8
1.134	0.0040	2	white solid	white powder	86.3
1.127	0.0040	4	white solid	white powder	94.8
1.134	0.0040	6	white solid	white powder	76.8
1.130	0.0040	9	white solid	white powder	86.5
1.122	0.0040	12	white solid	white powder	85.8
1.153	0.0041	24	white solid	white powder	92.8
1.112	0.0039	48	white solid	white powder	91.2
1.126	0.0040	72	white solid	white powder	87.6
1.128	0.0040	96	white solid	white powder	82.8

Table 3.19 : Polymerisations of ε-caprolactone at 100°C using boron trifluoride diethyl etherate as initiator.

Monomer (g)	Initiator (g)	Time (hrs.)	Physical Appearance of Product at Room Temp.		Conversion (%)
			Crude	Purified	
2.419	0.003	1	brown solid	brown powder	23.6
2.442	0.003	2	brown solid	brown powder	42.8
2.409	0.003	4	brown solid	brown powder	53.0
2.470	0.004	6	brown solid	brown powder	59.5
2.441	0.003	9	brown solid	brown powder	66.7
2.413	0.003	12	brown solid	brown powder	67.2
2.419	0.003	24	brown solid	brown powder	81.3
2.413	0.003	48	brown solid	brown powder	85.6
2.424	0.003	72	brown solid	brown powder	89.2
2.422	0.003	96	brown solid	brown powder	86.8

Table 3.20 : Polymerisations of ε-caprolactone at 150°C using boron trifluoride diethyl etherate as initiator.

Monomer (g)	Initiator (g)	Time (hrs.)	Physical Appearance of Product at Room Temp.		Conversion (%)
			Crude	Purified	
2.406	0.003	1	brown solid	brown powder	70.7
2.438	0.003	2	brown solid	brown powder	69.1
2.422	0.005	4	brown solid	brown powder	89.2
2.425	0.003	6	brown solid	brown powder	83.7
2.426	0.003	9	brown solid	brown powder	85.4
2.212	0.004	12	brown solid	brown powder	90.6
20413	0.003	24	brown solid	brown powder	83.3
3.258	0.004	48	brown solid	brown powder	90.0
3.202	0.004	72	brown solid	brown powder	90.9
2.410	0.003	96	brown solid	brown powder	89.6

Table 3.21 : Polymerisations of ε-caprolactone at 100°C using lithium *t*-butoxide as initiator.

Monomer (g)	Initiator (g)	Time (hrs.)	Physical Appearance of Product at Room Temp.		Conversion (%)
			Crude	Purified	
2.860	0.0020	1	brown solution	no solid ppte.	0
2.849	0.0020	2	brown solution	no solid ppte.	0
2.850	0.0020	4	brown solution	no solid ppte.	0
2.848	0.0020	6	brown solution	no solid ppte.	0
2.850	0.0020	9	brown solution	no solid ppte.	0
2.847	0.0020	12	brown solution	no solid ppte.	0
2.779	0.0021	24	brown solution	no solid ppte.	0
2.800	0.0020	48	brown solution	no solid ppte.	0
2.869	0.0020	72	brown solid	brown powder	0.2
2.894	0.0020	96	brown solid	brown powder	0.2

Table 3.22 : Polymerisations of ε-caprolactone at 150°C using lithium *t*-butoxide as initiator.

Monomer (g)	Initiator (g)	Time (hrs.)	Physical Appearance of Product at Room Temp.		Conversion (%)
			Crude	Purified	
2.859	0.0019	1	brown solution	no solid ppte.	0
2.849	0.0021	2	brown solution	no solid ppte.	0
2.849	0.0021	4	brown solution	no solid ppte.	0
2.860	0.0021	6	brown solution	no solid ppte.	0
2.859	0.0021	9	brown solution	no solid ppte.	0
2.849	0.0020	12	brown solid	brown powder	12.5
2.852	0.0020	24	brown solid	brown powder	55.4
2.858	0.0020	48	brown solid	brown powder	76.2
2.853	0.0020	72	brown solid	brown powder	86.6
2.858	0.0020	96	brown solid	brown powder	91.2

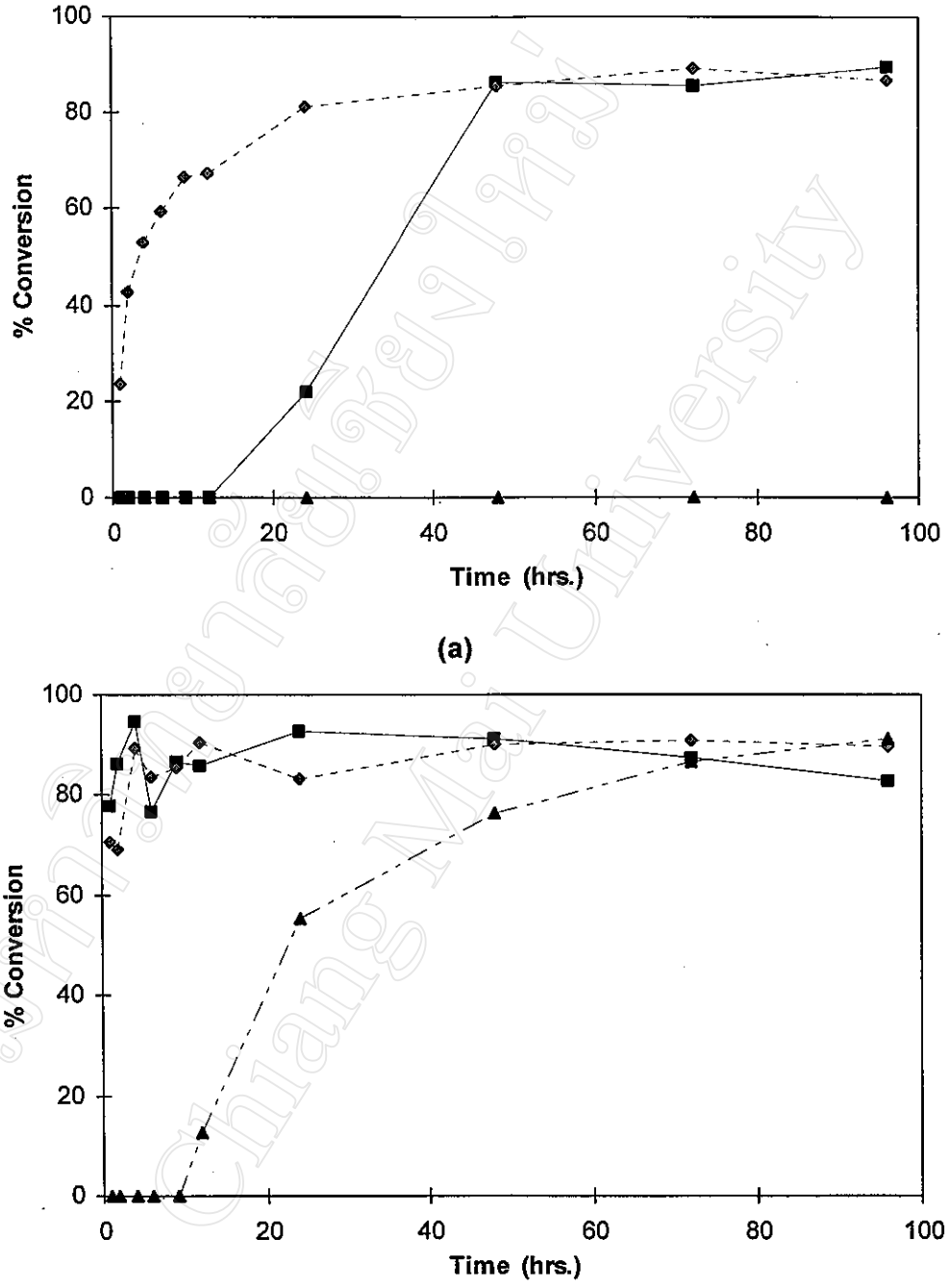

Fig. 3.10 : Comparison of ε-caprolactone conversion-time profiles using different initiators at (a) 100°C and (b) 150°C.

3.3.3 Polymer Characterisation

3.3.3.1 Chemical Structure

A typical infrared spectrum of one of the purified poly(ε-caprolactone) (PCL) products is shown in Fig. 3.11. The spectrum, which was obtained from a sample prepared in the form of a thin film cast from solution in chloroform, compares very closely with the reference spectrum in Fig. 3.12. The major vibrational peak assignments are listed below in Table 3.23.

Table 3.23 : Infrared absorption band assignments for poly(ε-caprolactone).

Vibrational Assignment	Band Intensity*	Wavenumber (cm^{-1})
O-H stretching, in OH / COOH end-groups	w	3600-3400
C-H stretching, in CH_2	m	2939, 2861
C=O stretching	s	1723
C-H bending, in CH_2	m	1470-1400
C-O stretching, acyl-oxygen	m	1250
C-O stretching, alkyl-oxygen	m	1060

* w = weak m = medium s = strong

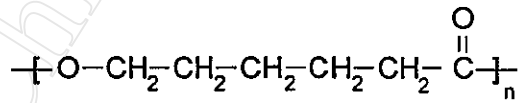

poly(ε-caprolactone), PCL

The PCL spectrum in Fig 3.11 is therefore seen to be consistent with the polymer's chemical structure. It is also worth noting that the O-H stretching peak in the region of 3400-3600 cm^{-1}, due to the presence of residual OH and/or COOH end-groups in the polymer, is extremely small for this particular sample. This is indicative of at least a reasonable level of molecular weight attainment, an indication confirmed by GPC analysis ($\overline{M}_n$ = 19070, $\overline{DP}_n$ = 167) as described later in section 3.3.3.4.

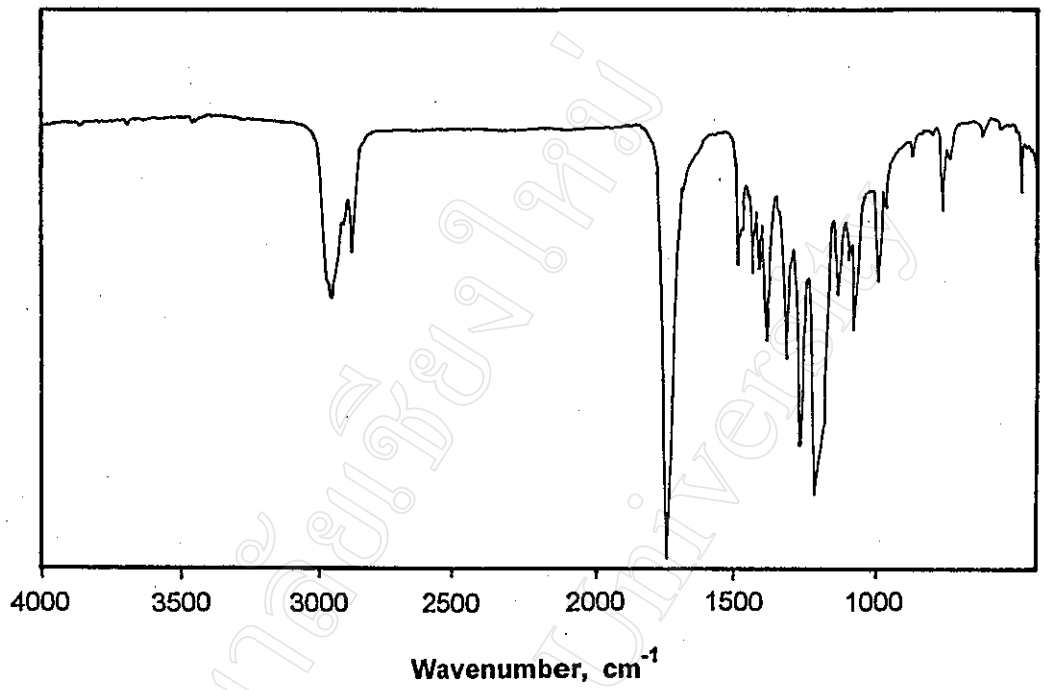

Fig. 3.11 : Infrared spectrum of purified poly(ε-caprolactone) synthesized at 150°C for 24 hours using stannous octoate as initiator.

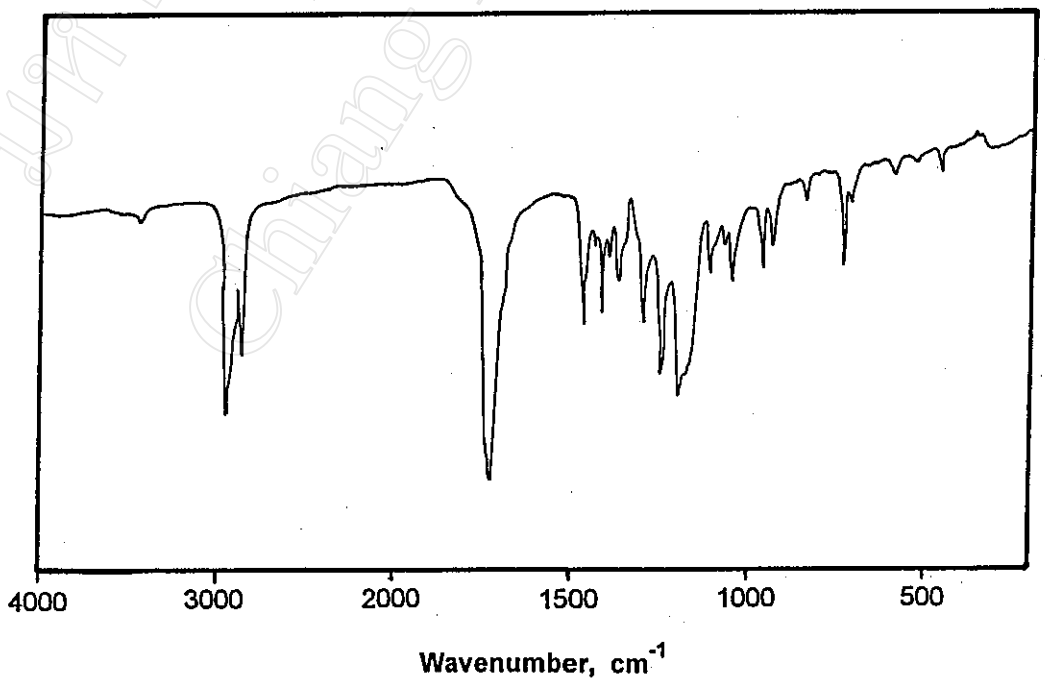

Fig 3.12 : Reference infrared spectrum of poly(ε-caprolactone) [82].

3.3.3.2 Temperature Transitions

A typical DSC curve for the purified PCL samples prepared in this work is illustrated in Fig. 3.13 showing the crystalline melting endotherm. The heat of melting (ΔH_m = 93.17 J/g) printed out on Fig. 3.13 is a measure of the polymer's % crystallinity. In the case of PCL, this % crystallinity can actually be calculated by comparison of ΔH_m with ΔH_m^* = 142 J/g, the theoretical heat of melting for a 100% crystalline PCL sample, as obtained from the literature [119].

$$\% \text{ crystallinity} = \frac{93.17 \text{ J/g}}{142 \text{ J/g}} \times 100\%$$

$$= 65.6\%$$

This relatively high value is partly a consequence of the fact that PCL's glass transition temperature ($T_g \approx -60^{\circ}C$) is well below ambient so that the polymer possesses sufficient molecular motion for crystallisation to occur quite easily at room temperature.

Also in Fig. 3.13, the polymer's melting peak temperature of 60.80°C, which is usually taken as its melting point, T_m (corrected to 61°C), is in close agreement with literature values for PCL (e.g., T_m = 63°C [84]). Apart from the melting transition, no other temperature transitions are evident in Fig. 3.13.

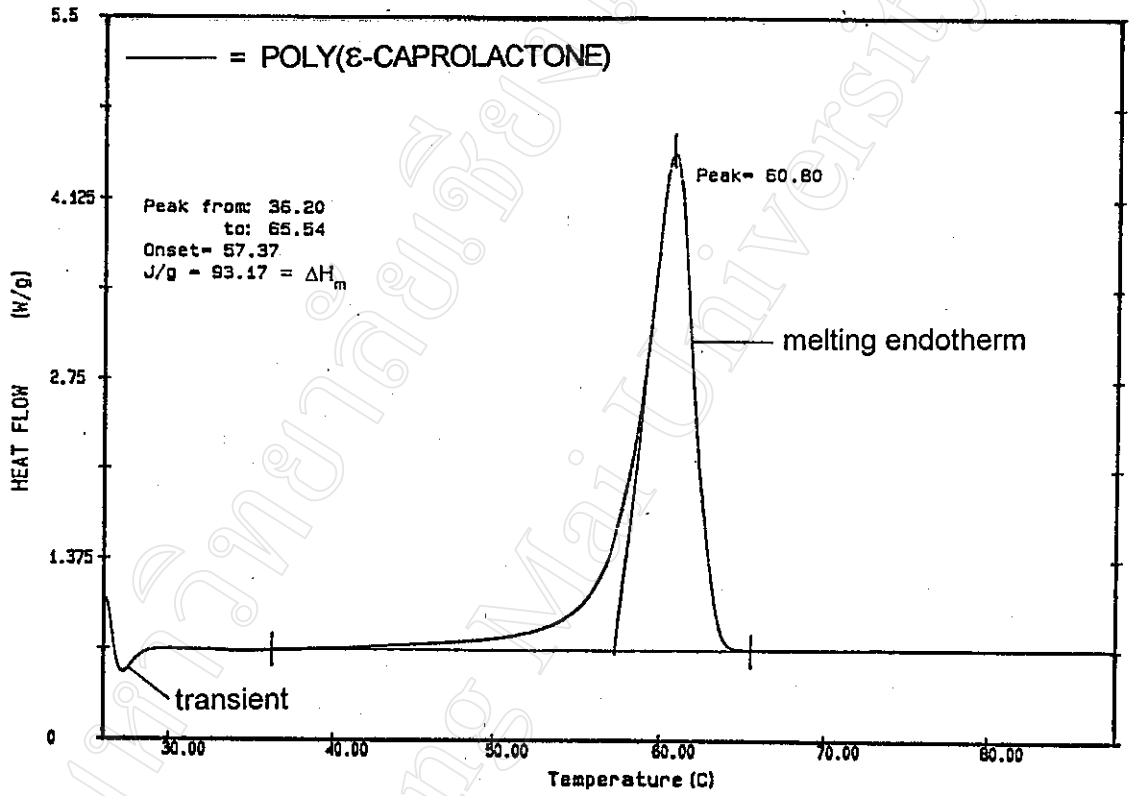

Fig. 3.13 : DSC thermogram of purified poly(ε-caprolactone) synthesized at 150°C for 24 hours using stannous octoate as initiator.

(Heating rate = 10°C/min; atmosphere = dry N_2)

3.3.3.3 Thermal Stability

A typical TG curve for the PCL synthesized here is shown in Fig. 3.14. The curve shows an essentially complete (>99%) weight loss over the temperature range 230-480°C. This confirms that PCL does indeed have a higher thermal stability than PVL (T_d range ≈ 190-390°C), as previously suggested, and would not be expected to decompose at the higher of the two polymerisation temperatures of 150°C.

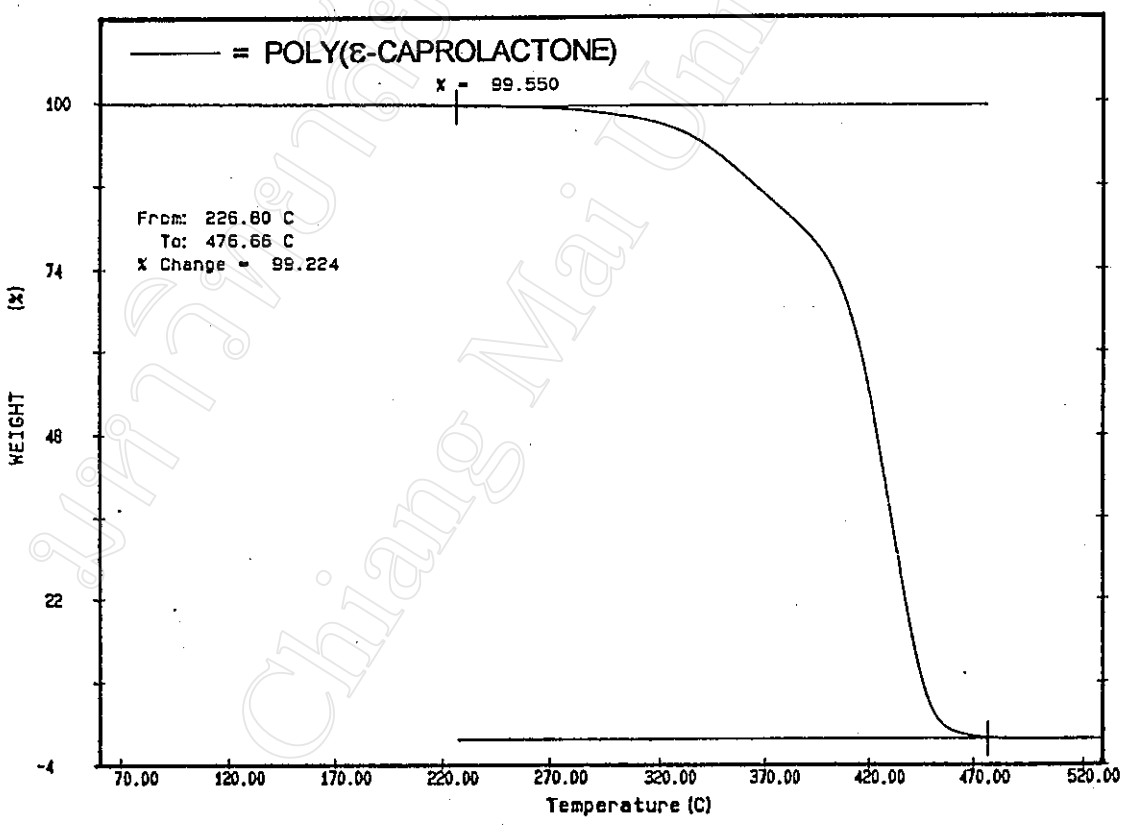

Fig. 3.14 : TG thermogram of purified poly(ε-caprolactone) synthesized at 150°C for 24 hours using stannous octoate as initiator.

(Heating rate = 20°C/min; atmosphere = dry N_2)

3.3.3.4 Molecular Weight

For this particular case of PCL, three different methods of molecular weight determination were employed so that the results for one sample only could be compared. Again, the main method used was gel permeation chromatography (GPC) because of its speed and convenience in measuring a large number of samples. However, in addition to GPC, vapour pressure osmometry and dilute-solution viscometry were also used for just one of the samples so that their $\overline{M}_n$ and $\overline{M}_v$ results respectively could be compared and checked against those obtained from GPC. PCL is one of the few polylactones for which the Mark-Houwink-Sakurada intrinsic viscosity-molecular weight relationship is reported in the literature.

(a) Gel Permeation Chromatography

GPC measurements were carried out in exactly the same way as described previously, using tetrahydrofuran as solvent at 30°C. The data print-out for the one PCL sample which was analysed by all three molecular weight methods is shown in Fig. 3.15. The GPC results for all of the samples are summarized in Tables 3.24-3.28 and plotted for ease of comparison in Fig. 3.16.

The molecular weight-time profiles in Fig. 3.16 are not greatly dissimilar from those for poly(δ-valerolactone) previously. Again, molecular weight build-up tends to follow % conversion with an apparent convergence towards some common limiting value at long reaction times. Whilst it is tempting to suggest that this is a logical consequence of the parity between the reaction parameters (same initiator concentration, same batch of monomer, etc.), it is probably not as simple as this. Transesterification reactions in the melt undoubtedly play a part, although to what extent is difficult to assess. This would require a separate set of degradation experiments. Suffice it to say that, from the results obtained in this work, the molecular weight profiles probably reflect the hidden balance with time and conversion between polymerisation on the one hand and transesterification on the other. Together, these competing processes determine the ultimate molecular weight attainable under any given set of reaction conditions.

TECHNICAL SERVICE, NATIONAL METAL AND MATERIALS TECHNOLOGY CENTER

Version 3.00a - MULTIDETECTOR GPC SOFTWARE - revised 03/17/93 J.Lesec

PCL/0.1%Sn(Oct)2/@150C/12hrs RESULTS Thu 21 AUG 1997 15:55:46
Polystyrene - 3 # 1 RUN # 5 Inj # 7 CODE : INJ 63
DATE : Thu 21 AUG 1997 TIME : 11:23:22 Manual integration
Calibration # 1.003 Number of points: 264 Axial dispersion: NO

MOLECULAR WEIGHTS UNIVERSAL

Peak mol. wt	Mp :	33920
Number aver.	Mn :	19070
Viscos. aver.	Mv :	32200
Weight averag.	Mw :	36540
Z average	Mz :	58220
Polydispersity	:	1.92
[n] (ml/g)	:	65.43
Log(K) (M-H)	:	-.5979
Alpha (M-H)	:	.535

REFRACTOMETER C/c : 1 Peak elution : 15.696 Baseline : .099688
Area constant : 2.211 Conc. (g/ml) : .0038 dn/dc : 0
VISCOMETER Mn : 3087 Peak elution : 15.457 Baseline : .89345
[n]area (ml/g): 68.62 [n]peak(ml/g): 78.26 [n]exp (ml/g): 65.43

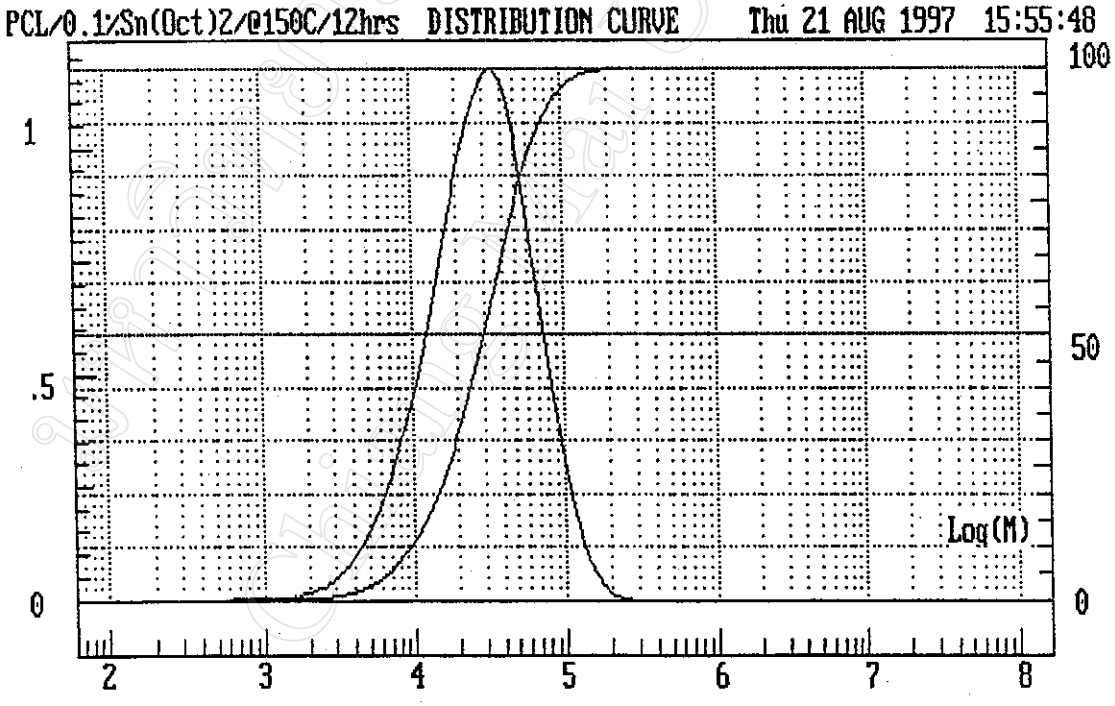

Fig. 3.15 : GPC curves and data print-out for purified poly(ε-caprolactone) synthesized at 150°C for 12 hours using stannous octoate as initiator.

Table 3.24 : GPC molecular weight averages and polydispersity indices for the PCL synthesized at 100°C using stannous octoate as initiator.

Polymerisation Time (hrs.)	Molecular Weight Averages			$\bar{M}_w / \bar{M}_n$
	$\bar{M}_n$	$\bar{M}_v$	$\bar{M}_w$	
24	3604	4524	4976	1.38
48	5590	7521	8510	1.52
72	7344	10080	11060	1.51
96	10400	15410	17020	1.64

Table 3.25 : GPC molecular weight averages and polydispersity indices for the PCL synthesized at 150°C using stannous octoate as initiator.

Polymerisation Time (hrs.)	Molecular Weight Averages			$\bar{M}_w / \bar{M}_n$
	$\bar{M}_n$	$\bar{M}_v$	$\bar{M}_w$	
1	16590	28860	32570	1.96
2	23690	40430	45780	1.93
4	19240	33490	38960	2.03
6	23290	35820	39850	1.71
9	14110	24650	28320	2.01
12	19070	32200	36540	1.92
24	12880	22810	25940	2.01
48	12300	20970	23920	1.94
72	9856	15430	18390	2.05
96	8634	14080	16710	1.94

Table 3.26 : GPC molecular weight averages and polydispersity indices for the PCL synthesized at 100°C using boron trifluoride diethyl etherate as initiator.

Polymerisation Time (hrs.)	Molecular Weight Averages			$\bar{M}_w / \bar{M}_n$
	$\bar{M}_n$	$\bar{M}_v$	$\bar{M}_w$	
1	5547	6935	7658	1.38
2	7613	9944	10870	1.43
4	9769	12980	13780	1.41
6	8520	11960	13520	1.59
9	8113	12030	13730	1.69
12	9839	13780	15280	1.55
24	10370	19400	24050	2.32
48	16490	27420	30750	1.87
72	12230	20120	22760	1.86
96	8170	12220	13690	1.68

Table 3.27 : GPC molecular weight averages and polydispersity indices for the PCL synthesized at 150°C using boron trifluoride diethyl etherate as initiator.

Polymerisation Time (hrs.)	Molecular Weight Averages			$\bar{M}_w / \bar{M}_n$
	$\bar{M}_n$	$\bar{M}_v$	$\bar{M}_w$	
1	6938	10820	12900	1.86
2	7246	10610	11990	1.65
4	7736	11690	13670	1.77
6	9498	13570	14980	1.58
9	9133	12980	14020	1.54
12	8298	12440	14080	1.70
24	11900	18990	20990	1.76
48	8467	14500	17440	2.06
72	9728	19660	26110	2.68
96	7982	15830	20630	2.58

Table 3.28 : GPC molecular weight averages and polydispersity indices for the PCL synthesized at 150°C using lithium *t*-butoxide as initiator.

Polymerisation Time (hrs.)	Molecular Weight Averages			$\bar{M}_w / \bar{M}_n$
	$\bar{M}_n$	$\bar{M}_v$	$\bar{M}_w$	
24	5955	7542	8217	1.38
48	9853	13710	15180	1.54
72	10780	17130	19440	1.80
96	11180	17770	19550	1.75

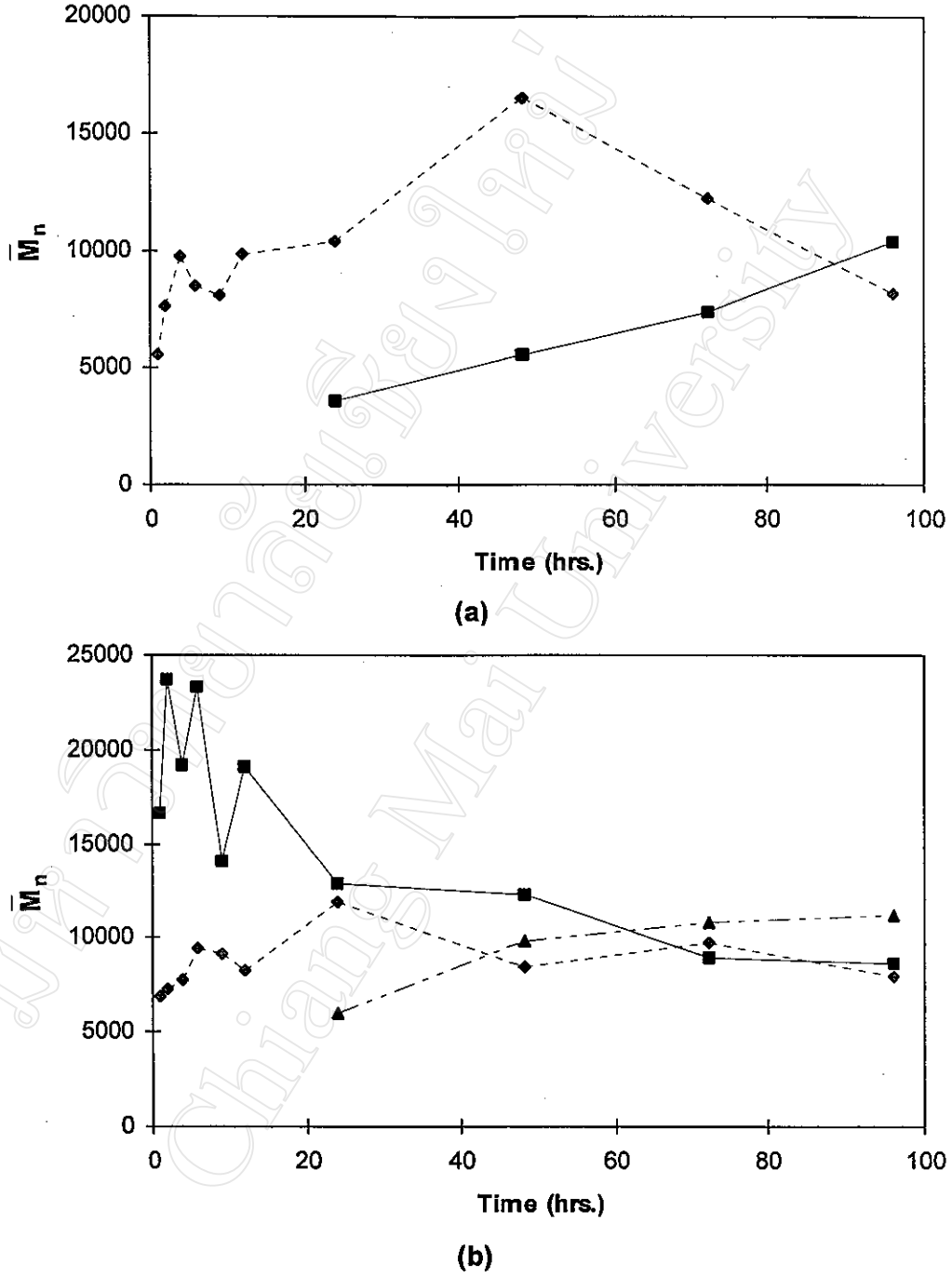

Fig. 3.16 : Comparison of PCL number-average molecular weight $\bar{M}_n$-time profiles using different initiators at (a) 100°C and (b) 150°C.

(b) Vapour Pressure Osmometry

The standard analytical procedure, as described previously in section 2.3.7 on pages 93-95, was based on the following conditions:

thermistor probe	: universal bead thermistor (25-75°C)
calibration standard	: tristearin (mol.wt. = 891.51)
solvent	: distilled chloroform ($CHCl_3$)
temperature	: 45.0°C
sensitivity	: 32
concentration range	: 3-15 g/kg solvent

The molecular weight calibration standard, tristearin, was dissolved in the $CHCl_3$ solvent at ambient temperature and then heated in the osmometer at 45.0°C for about 30 minutes. The solution of lowest concentration was measured first, as soon as temperature equilibrium had been attained. Measurements were recorded after 2 minutes and repeated every 30 seconds in order to determine the most reliable value for the balancing resistance (ΔR). This was eventually taken as the mean of the most 3 similar readings. The results are summarized in Table 3.29 below.

Table 3.29 : Balancing resistance (ΔR) for different solution concentrations of tristearin (calibrant) in $CHCl_3$ at 45.0°C.

Concentration (g/kg)	ΔR* (scd)	ΔR/c (scd·kg/g)
3.539	9.0	2.54
5.380	12.4	2.30
6.868	16.5	2.40
10.262	25.0	2.44
14.206	32.5	2.29

* = mean of the 3 most similar readings

scd = scale divisions (as read from the measuring instrument)

The calibration constant, K, is calculated from the results in Table 3.29 by plotting the graphs shown in Fig. 3.17. Then, knowing the limiting value of ($\Delta R/c$) at c = 0 in the equation :

$$(\Delta R / c)_{c=0} = K / \bar{M}_n$$

and replacing $\bar{M}_n$ by M (molecular weight of the tristearin standard), the equation becomes

$$(\Delta R / c)_{c=0} = K / M$$

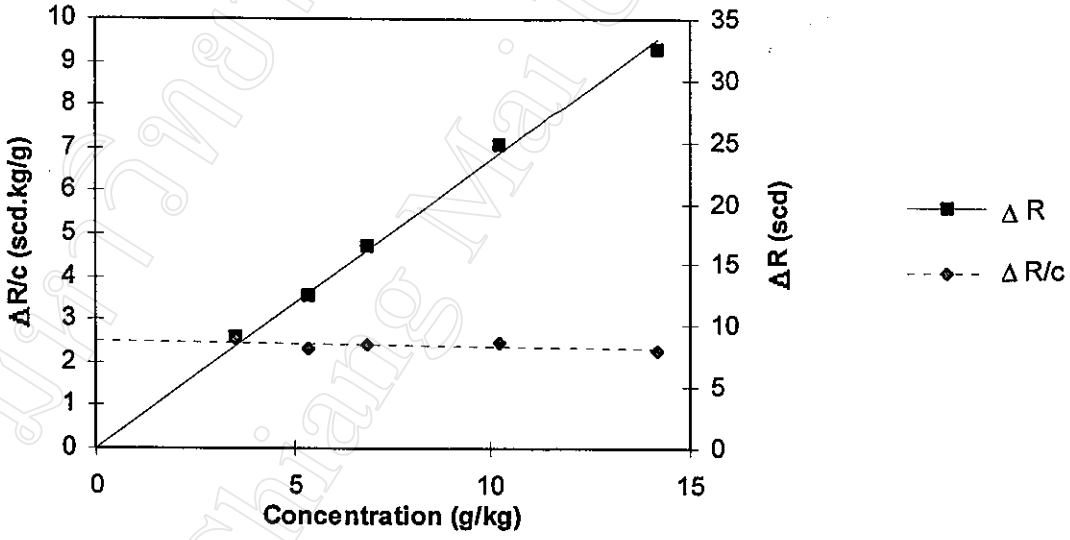

Fig. 3.17 : Extrapolation of ΔR and $\Delta R/c$ to infinite dilution (c=0) for the standard solutions of tristearin in $CHCl_3$ at 45.0°C.

From Fig. 3.17, $(\Delta R / c)_{c=0}$ of tristearin = 2.50 scd·kg/g

molecular weight of tristearin = M = 891.51 g/mol

Therefore,

$$K = 2.23 \times 10^3 \text{ scd·kg/mol}$$

For purposes of comparison, the PCL sample chosen for this analysis was the same as that for which the GPC curves were shown previously in Fig. 3.15, i.e. that synthesized at 150°C for 12 hours using $Sn(Oct)_2$ as initiator. The conditions used and results obtained were as follows:

thermistor probe	: universal bead thermistor (25-75°C)
PCL sample	: synthesised at 150°C for 12 hours using $Sn(Oct)_2$ as initiator
solvent	: distilled chloroform ($CHCl_3$)
temperature	: 45.0°C
sensitivity	: 128
concentration range	: 1-9 g/kg solvent

Table 3.30 : Balancing resistance (ΔR) for different solution concentrations of PCL in $CHCl_3$ at 45.0°C.

Concentration (g/kg)	ΔR* (scd)	ΔR/c (scd·kg/g)
1.836	0.8	0.44
3.060	1.4	0.45
5.099	2.4	0.47
8.499	4.0	0.47

* = mean of the 3 most similar readings

scd = scale divisions (as read from the measuring instrument)

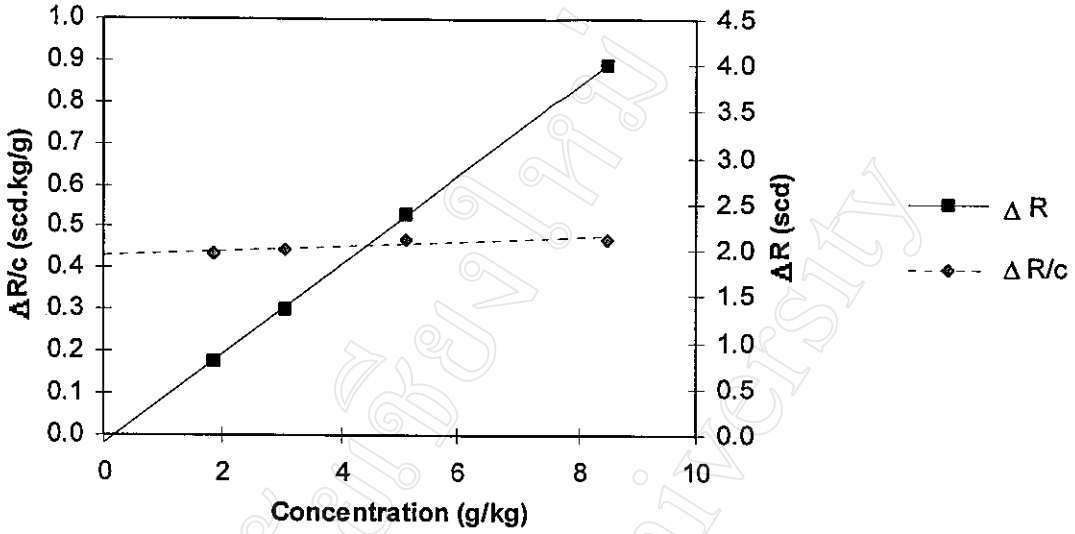

Fig. 3.18 : Extrapolation of ΔR and ΔR/c to infinite dilution (c=0) for the PCL sample solutions in $CHCl_3$ at 45.0°C.

The value of the polymer's number-average molecular weight, $\bar{M}_n$, is now calculated using the previous calibration constant, K = 2.23 x 10^3 scd·kg/g, and, from Fig. 3.18, the limiting value of

$$(\Delta R / c)_{c=0} = 0.43 \text{ scd} \cdot \text{kg} / \text{g}$$

Therefore, for this PCL sample, from $(\Delta R / c)_{c=0} = K/\bar{M}_n$

$$\bar{M}_n = 20700 \text{ g/mol}$$

This value of $\bar{M}_n$ = 20700 from vapour pressure osmometry compares favourably with the previously value of $\bar{M}_n$ = 19070 from GPC (Fig. 3.15). Since osmometry is an absolute method for polymer molecular weight determination, this result serves to enhance the confidence level in the GPC data upon which the molecular weight conclusions in this work are based.

(c) Dilute-Solution Viscometry

The viscometric flow-time data and derived viscosity parameters relating to the same PCL sample, synthesized at 150°C for 12 hours using $Sn(Oct)_2$ as initiator, are given in Table 3.31 below. The measurements were made in THF solution at 30°C.

Table 3.31 : Dilute-solution viscosity data and calculated viscosity terms for PCL in THF at 30°C.

Concentration c (g/dl)	Average Flow-Time t (sec.)	η_{rel}	η_{sp}	η_{red} (dl/g)	η_{inh} (dl/g)
0	164.9	-	-	-	-
0.126	177.7	1.077	0.077	0.614	0.592
0.249	190.3	1.154	0.154	0.632	0.574
0.739	246.1	1.492	0.492	0.666	0.542
1.024	278.2	1.688	0.688	0.671	0.511

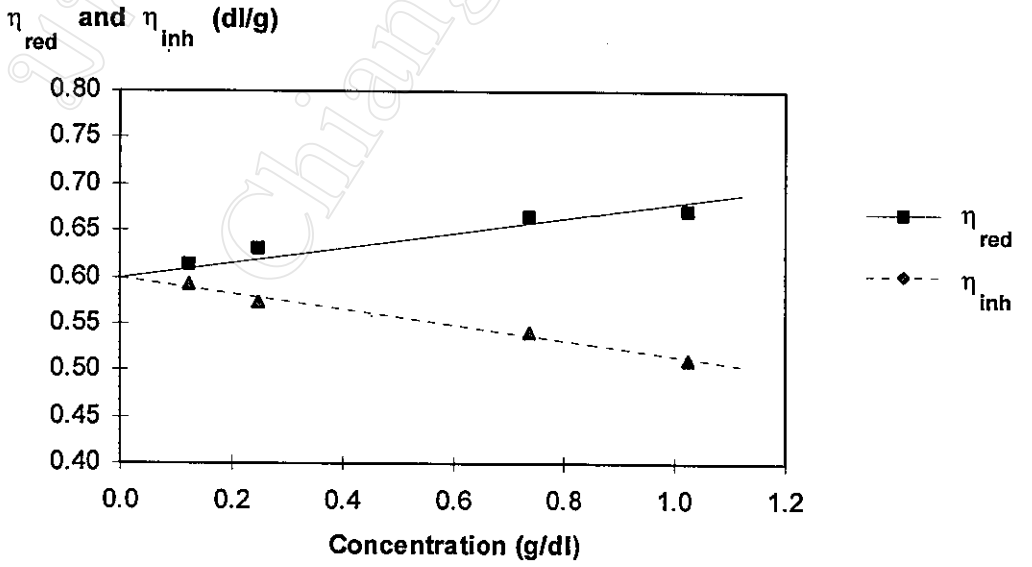

Fig. 3.19 : Graphs of reduced and inherent viscosity against concentration for PCL in THF at 30°C.

On plotting the reduced viscosity (η_{red}) and inherent viscosity (η_{inh}) against concentration, as shown in Fig. 3.19, and double extrapolating to zero concentration, a value for the intrinsic viscosity [η] of the PCL sample of 0.60 dl/g is obtained. From this vale of [η], the polymer's viscosity-average molecular weight, $\bar{M}_v$, can be calculated from the following Mark-Houwink-Sakurada Equation for PCL in THF as solvent at 30°C [120]:

$$[\eta] = 1.40 \times 10^{-4} \bar{M}_v^{0.79} \text{ dl/g}$$

$$\bar{M}_v = 39600$$

These values of [η] = 0.60 dl/g and $\bar{M}_v$ = 39600 from dilute-solution viscosity, like the osmometry results previously, also compare favourably with the corresponding values of [η] = 0.65 dl/g and $\bar{M}_v$ = 32200 from GPC (Fig. 3.15). The fact that these two alternative methods have yielded molecular weight averages in such close agreement serves to reaffirm the reliability of the GPC values. These molecular weight values from the three methods are summarized in Table 3.32.

Table 3.32 : Comparison of molecular weight averages obtained from three different methods for the same PCL sample.

Experimental Method	$\bar{M}_n$	$\bar{M}_v$
Gel Permeation Chromatography	19070	32200
Vapour Pressure Osmometry	20700	-
Dilute-Solution Viscometry	-	39600

3.4 Glycolide

3.4.1 Polymerisation Procedure

The 6-membered ring glycolide, with its ester difunctionality, is well known to be extremely reactive towards polymerisation. Indeed, it polymerises spontaneously on melting at just over 80°C. However, it has the disadvantage of being highly hygroscopic and easily hydrolysable to the parent glycolic acid. Glycolide is one of the most widely studied cyclic ester monomers. Its polymer, poly(glycolic acid) (PGA) has been widely used for a long time in biomedical applications where its biodegradability is advantageous, e.g. in absorbable surgical sutures. Structurally, it is the simplest polyester with an exceptionally high melting point of around 220°C.

For glycolide, the series of polymerisation experiments that were carried out in this work are summarized in Table 3.33. The polymerisation procedure was the same as that described in the previous sections except that, in addition:

(a) A higher temperature of 180°C was also studied because of PGA's exceptionally high melting point.

(b) Glycolide was accurately weighed into a 25 ml conical flask with a magnetic stirrer (see Fig. 3.20).

(c) At the end of each polymerisation period, the flask was allowed to cool to room temperature. The poly(glycolic acid), PGA, product was then ground up into a fine powder and refluxed in absolute ethanol with efficient stirring at 77-78°C for 10 hours, as shown in Fig. 3.21. The purified polymer was filtered off, washed with more hot ethanol and dried to constant weight in a vacuum oven at 60°C. The purified products obtained are each described in Tables 3.34-3.42.

The reason why the crude PGA was purified by hot alcohol extraction rather than by reprecipitation was because of its insolubility in all common organic solvents. The only effective solvents were hot dimethylsulphoxide (DMSO) and hot benzyl alcohol, each of which had the disadvantage of being potentially interactive and also

very difficult to remove from the reprecipitated polymer. Thus, hot alcohol extraction was used instead to remove any remaining monomer and initiator residues.

3.4.2 Polymerisation Results

The most striking aspect of the glycolide polymerisation profiles in Fig. 3.22 is the much faster rates of polymerisation which are attainable compared with the previous 3 lactone monomers. This is especially evident at the 2 higher reaction temperatures of 150°C and 180°C, conversions being essentially quantitative within the first 6 hours. This clearly demonstrates the high reactivity of the glycolide ring.

The much slower rates at 100°C are probably as much a result of solidification of the polymerisate as of the lower temperature. Unlike the previous polylactones which all had low melting points (< 70°C), PGA has a much higher melting point of around 220°C. Consequently, when glycolide polymerisations are carried out at temperatures below 200°C, the polymer product solidifies as and when a certain molecular weight level is attained. The lower the reaction temperature, the faster it solidifies or, to express it another way, the shorter the time that the polymerisate can remain mobile in the melt state. This has implications for both the polymerisation kinetics and the molecular weight build-up since the reaction, to a large extent, is "frozen" in the solid state. This effect is reflected in the 2 conversion-time profiles in Fig. 3.22(a) for the slower $Sn(Oct)_2$ and Li(*t*-OBu)-initiated reactions which show clearly how the reactions are stalled by solidification.

The other point of interest in Fig. 3.22 is the $BF_3{\cdot}Et_2O$-intiated reaction profile in Fig. 3.22(c). Generally, $BF_3{\cdot}Et_2O$ gives the fastest rate of all the initiators but, at the highest temperature of 180°C, it appears to give the slowest. This is thought to be due to partial loss of the $BF_3{\cdot}Et_2O$ complex from the polymerisate by volatilisation since its boiling point of 126°C (manufacturer's data) is well below the reaction temperature.

Table 3.33 : Summary of glycolide polymerisation experiments.

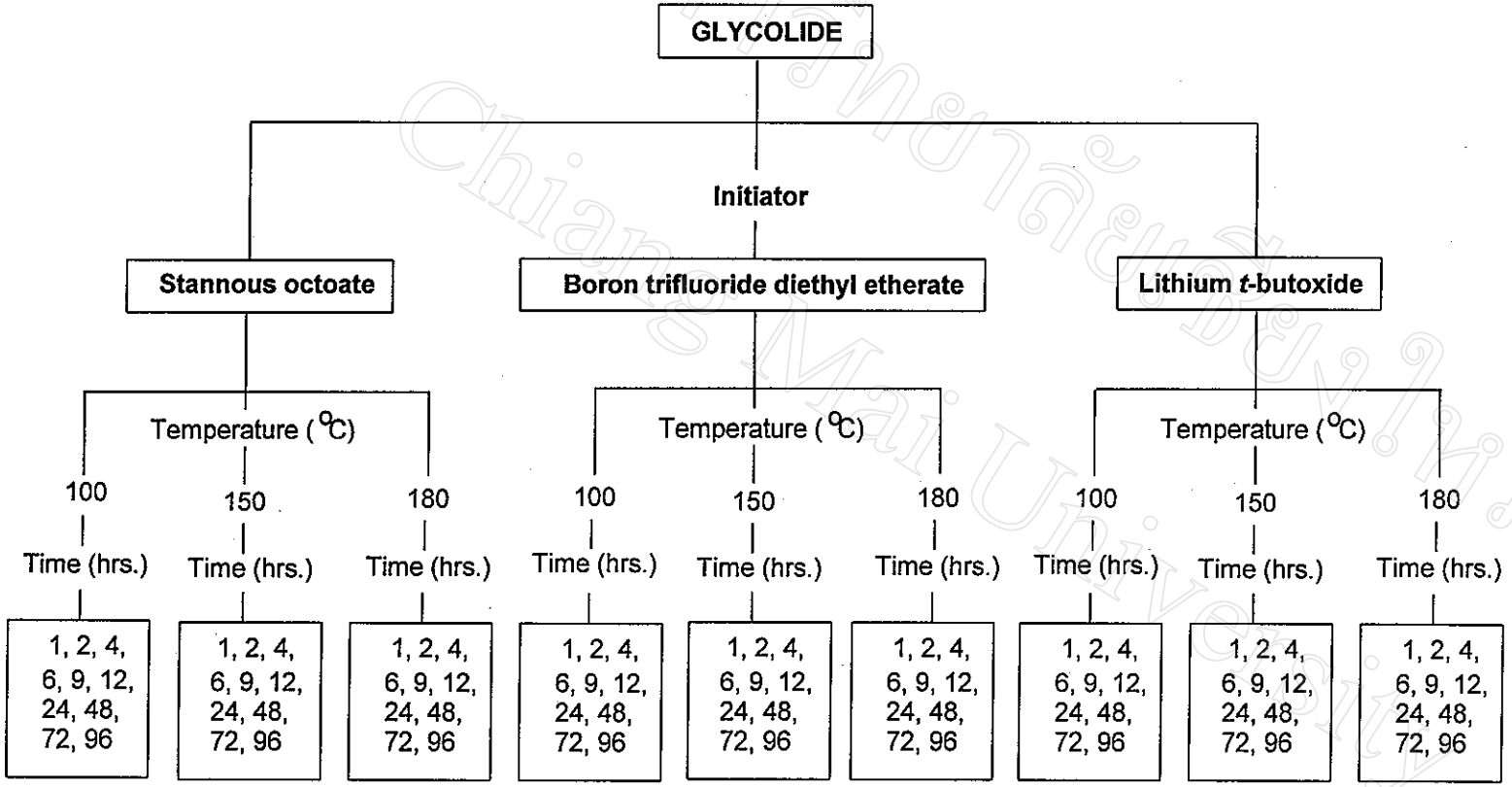

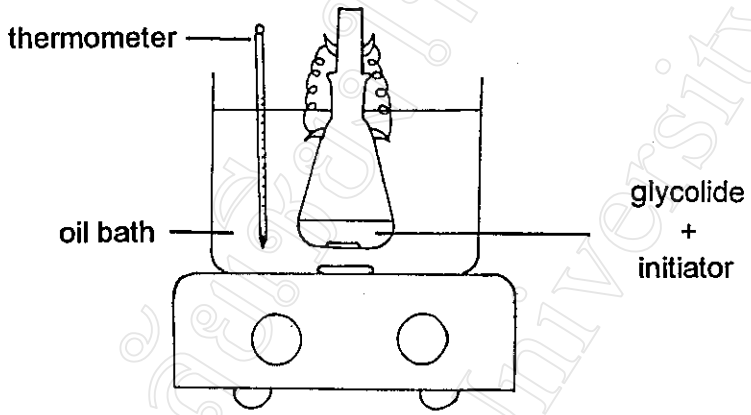

Fig. 3.20 : Apparatus used for the ring-opening polymerisation of glycolide.

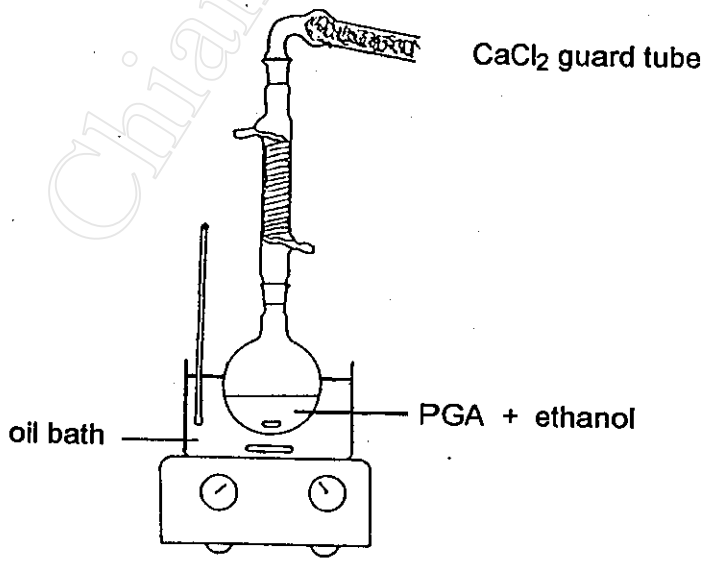

Fig. 3.21 : Apparatus used for the purification of crude PGA by hot ethanol extraction.

Table 3.34 : Polymerisations of glycolide at 100°C using stannous octoate as initiator.

Monomer (g)	Initiator (g)	Time (hrs.)	Physical Appearance of Product at Room Temp.		Conversion (%)
			Crude	Purified	
1.148	0.0040	1	white solid	white powder	9.8
1.155	0.0040	2	white solid	white powder	10.6
1.158	0.0041	4	white solid	white powder	13.9
1.146	0.0039	6	white solid	white powder	16.3
1.142	0.0041	9	white solid	white powder	18.6
1.151	0.0041	12	white solid	white powder	20.7
1.140	0.0040	24	white solid	white powder	27.8
1.141	0.0040	48	white solid	white powder	32.3
1.154	0.0040	72	white solid	white powder	35.0
1.165	0.0040	96	white solid	white powder	33.4

Table 3.35 : Polymerisations of glycolide at 150°C using stannous octoate as initiator.

Monomer (g)	Initiator (g)	Time (hrs.)	Physical Appearance of Product at Room Temp.		Conversion (%)
			Crude	Purified	
1.148	0.0040	1	fawn-coloured solid	fawn-coloured solid	100.0
1.159	0.0041	2	fawn-coloured solid	fawn-coloured solid	99.5
1.153	0.0041	4	fawn-coloured solid	fawn-coloured solid	100.0
1.153	0.0040	6	fawn-coloured solid	fawn-coloured solid	99.8
1.143	0.0041	9	fawn-coloured solid	fawn-coloured solid	99.6
1.170	0.0040	12	fawn-coloured solid	fawn-coloured solid	100.0
1.169	0.0040	24	fawn-coloured solid	fawn-coloured solid	99.1
1.154	0.0041	48	fawn-coloured solid	fawn-coloured solid	99.7
1.151	0.0041	72	fawn-coloured solid	fawn-coloured solid	99.7
1.150	0.0041	96	fawn-coloured solid	fawn-coloured solid	100.0

Table 3.36 : Polymerisations of glycolide at 180°C using stannous octoate as initiator.

Monomer (g)	Initiator (g)	Time (hrs.)	Physical Appearance of Product at Room Temp.		Conversion (%)
			Crude	Purified	
1.145	0.0039	1	fawn-coloured solid	fawn-coloured solid	99.7
1.149	0.0040	2	fawn-coloured solid	fawn-coloured solid	99.5
1.146	0.0040	4	fawn-coloured solid	fawn-coloured solid	99.9
1.154	0.0041	6	fawn-coloured solid	fawn-coloured solid	99.0
1.139	0.0039	9	fawn-coloured solid	fawn-coloured solid	99.6
1.143	0.0040	12	fawn-coloured solid	fawn-coloured solid	99.8
1.153	0.0041	24	fawn-coloured solid	fawn-coloured solid	99.8
1.155	0.0041	48	fawn-coloured solid	fawn-coloured solid	100.0
1.158	0.0041	72	fawn-coloured solid	fawn-coloured solid	100.0
1.151	0.0041	96	fawn-coloured solid	fawn-coloured solid	99.6

Table 3.37 : Polymerisations of glycolide at 100°C using boron trifluoride diethyl etherate as initiator.

Monomer (g)	Initiator (g)	Time (hrs.)	Physical Appearance of Product at Room Temp.		Conversion (%)
			Crude	Purified	
1.651	0.002	1	fawn-coloured solid	fawn-coloured powder	14.7
1.643	0.002	2	fawn-coloured solid	fawn-coloured solid	15.9
1.645	0.002	4	fawn-coloured solid	fawn-coloured solid	16.3
1.644	0.002	6	fawn-coloured solid	fawn-coloured solid	17.1
2.465	0.003	9	fawn-coloured solid	fawn-coloured solid	31.2
1.644	0.002	12	fawn-coloured solid	fawn-coloured solid	36.8
1.645	0.002	24	fawn-coloured solid	fawn-coloured solid	46.6
1.642	0.002	48	fawn-coloured solid	fawn-coloured solid	94.0
2.456	0.003	72	fawn-coloured solid	fawn-coloured solid	96.9
1.640	0.002	96	fawn-coloured solid	fawn-coloured solid	92.9

Table 3.38 : Polymerisations of glycolide at 150°C using boron trifluoride diethyl etherate as initiator.

Monomer (g)	Initiator (g)	Time (hrs.)	Physical Appearance of Product at Room Temp.		Conversion (%)
			Crude	Purified	
1.634	0.002	1	fawn-coloured solid	fawn-coloured powder	44.1
1.642	0.002	2	fawn-coloured solid	fawn-coloured solid	96.3
1.635	0.002	4	fawn-coloured solid	fawn-coloured solid	88.9
1.640	0.002	6	fawn-coloured solid	fawn-coloured solid	100.0
1.632	0.002	9	fawn-coloured solid	fawn-coloured solid	99.6
1.656	0.002	12	fawn-coloured solid	fawn-coloured solid	99.0
2.447	0.003	24	fawn-coloured solid	fawn-coloured solid	100.0
1.641	0.002	48	fawn-coloured solid	fawn-coloured solid	99.6
1.639	0.002	72	fawn-coloured solid	fawn-coloured solid	99.8
1.655	0.002	96	fawn-coloured solid	fawn-coloured solid	99.6

Table 3.39 : Polymerisations of glycolide at 180°C using boron trifluoride diethyl etherate as initiator.

Monomer (g)	Initiator (g)	Time (hrs.)	Physical Appearance of Product at Room Temp.		Conversion (%)
			Crude	Purified	
1.642	0.002	1	brown solid	brown powder	15.6
2.450	0.003	2	brown solid	brown powder	54.7
1.636	0.002	4	brown solid	brown solid	73.2
1.632	0.002	6	brown solid	brown solid	98.2
1.632	0.002	9	brown solid	brown solid	98.5
1.635	0.002	12	brown solid	brown solid	98.9
1.641	0.002	24	brown solid	brown solid	99.5
1.633	0.002	48	brown solid	brown solid	99.5
1.642	0.002	72	brown solid	brown solid	98.9
1.633	0.002	96	brown solid	brown solid	99.6

Table 3.40 : Polymerisations of glycolide at 100°C using lithium *t*-butoxide as initiator.

Monomer (g)	Initiator (g)	Time (hrs.)	Physical Appearance of Product at Room Temp.		Conversion (%)
			Crude	Purified	
1.460	0.0011	1	fawn-coloured solid	fawn-coloured powder	12.6
1.447	0.0011	2	fawn-coloured solid	fawn-coloured powder	8.4
1.455	0.0010	4	fawn-coloured solid	fawn-coloured solid	16.7
1.462	0.0010	6	fawn-coloured solid	fawn-coloured solid	11.9
1.451	0.0011	9	fawn-coloured solid	fawn-coloured solid	21.3
1.458	0.0011	12	fawn-coloured solid	fawn-coloured solid	14.6
1.459	0.0010	24	fawn-coloured solid	fawn-coloured solid	19.8
1.544	0.0010	48	fawn-coloured solid	fawn-coloured solid	21.2
1.450	0.0011	72	fawn-coloured solid	fawn-coloured solid	21.2
1.454	0.0011	96	fawn-coloured solid	fawn-coloured solid	27.2

Table 3.41 : Polymerisations of glycolide at 150°C using lithium *t*-butoxide as initiator.

Monomer (g)	Initiator (g)	Time (hrs.)	Physical Appearance of Product at Room Temp.		Conversion (%)
			Crude	Purified	
1.448	0.0010	1	brown solid	brown powder	53.6
1.451	0.0010	2	brown solid	brown solid	86.5
1.466	0.0011	4	brown solid	brown solid	99.8
1.455	0.0010	6	brown solid	brown solid	100.0
1.461	0.0010	9	brown solid	brown solid	100.0
1.451	0.0010	12	brown solid	brown solid	99.8
1.454	0.0010	24	brown solid	brown solid	100.0
1.462	0.0011	48	brown solid	brown solid	100.0
1.450	0.0010	72	brown solid	brown solid	100.0
1.450	0.0010	96	brown solid	brown solid	99.9

Table 3.42 : Polymerisations of glycolide at 180°C using lithium *t*-butoxide as initiator.

Monomer (g)	Initiator (g)	Time (hrs.)	Physical Appearance of Product at Room Temp.		Conversion (%)
			Crude	Purified	
1.458	0.0011	1	dark brown solid	dark brown solid	99.0
1.454	0.0011	2	dark brown solid	dark brown solid	99.5
1.443	0.0011	4	dark brown solid	dark brown solid	99.0
1.448	0.0010	6	dark brown solid	dark brown solid	98.7
1.466	0.0011	9	dark brown solid	dark brown solid	99.3
1.448	0.0011	12	dark brown solid	dark brown solid	99.0
1.456	0.0010	24	dark brown solid	dark brown solid	99.1
1.452	0.0010	48	dark brown solid	dark brown solid	99.7
1.463	0.0011	72	dark brown solid	dark brown solid	99.7
1.448	0.0011	96	dark brown solid	dark brown solid	99.6

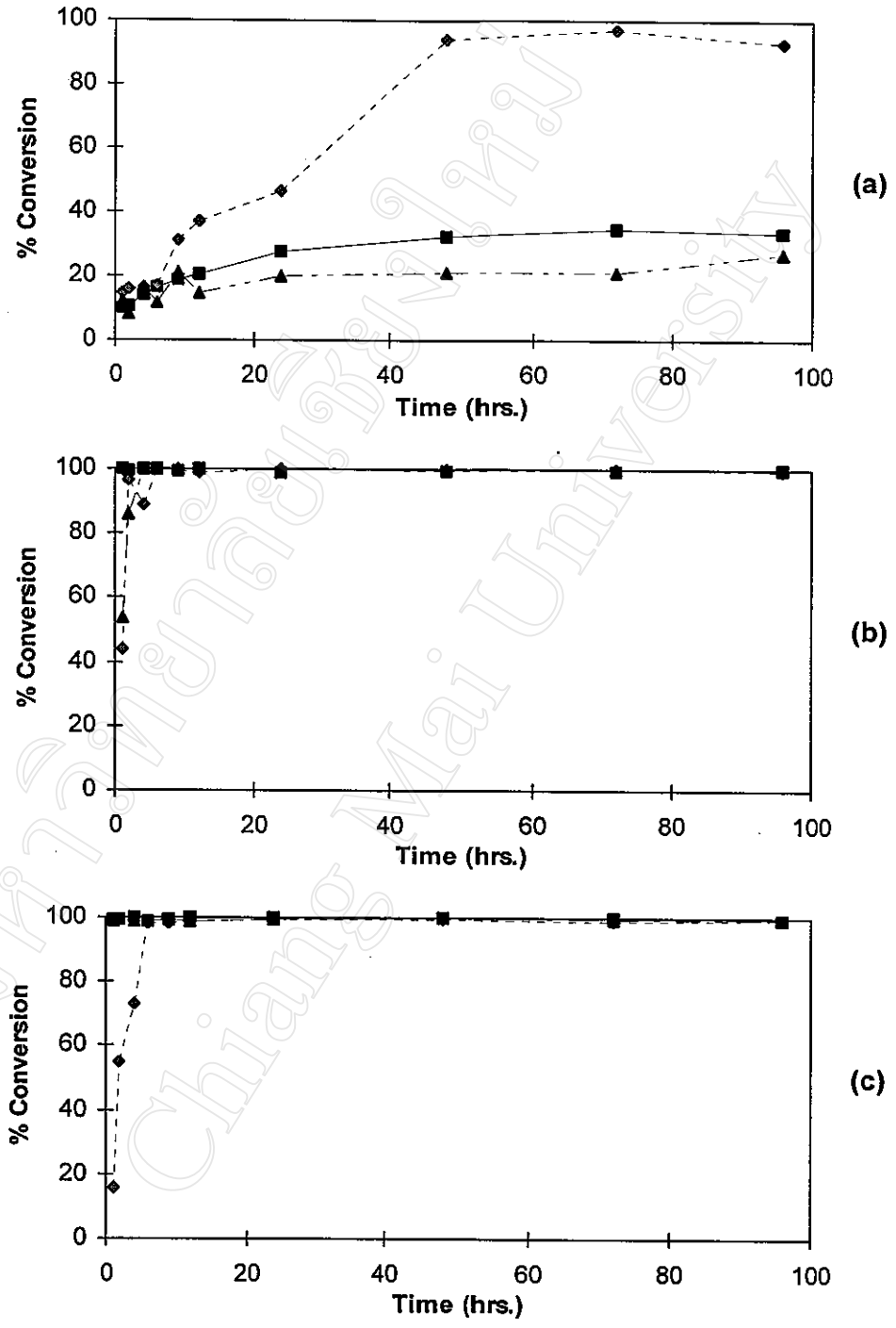

Fig. 3.22 : Comparison of glycolide conversion-time profiles using different initiators at (a) 100°C (b) 150°C and (c) 180°C.

—■— $Sn(Oct)_2$
- -◆- - $BF_3{\cdot}Et_2O$
—▲- - Li(*t*-OBu)

3.4.3 Polymer Characterisation

3.4.3.1 Chemical Structure

A typical infrared spectrum of one of the purified poly(glycolic acid) (PGA) products is shown in Fig. 3.23. The spectrum, which was obtained from a sample prepared in the form of KBr disc, can be compared with the reference spectrum in Fig. 3.24. The major vibrational peak assignments are listed in Table 3.43.

Table 3.43 : Infrared absorption band assignments for poly(glycolic acid).

Vibrational Assignment	Band Intensity*	Wavenumber (cm^{-1})
O-H stretching, in OH / COOH end-groups	m	3700-3300
C-H stretching, in CH_2	m	2980
C=O stretching	s	1745
C-H bending, in CH_2	s	1450-1400
C-O stretching, acyl-oxygen	m	1240
C-O stretching, alkyl-oxygen	m	1082

* w = weak m = medium s = strong

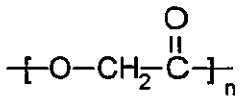

poly(glycolic acid), PGA

The PGA spectrum in Fig 3.23 is therefore seen to be consistent with the polymer's chemical structure. It is also worth noting that the O-H stretching peak in the region of 3700-3300 cm^{-1}, due to the presence of residual OH and/or COOH end-groups in the polymer, is significantly larger than for the previous polylactones. This is thought to be due to PGA's hygroscopic nature rather than an especially low molecular weight.

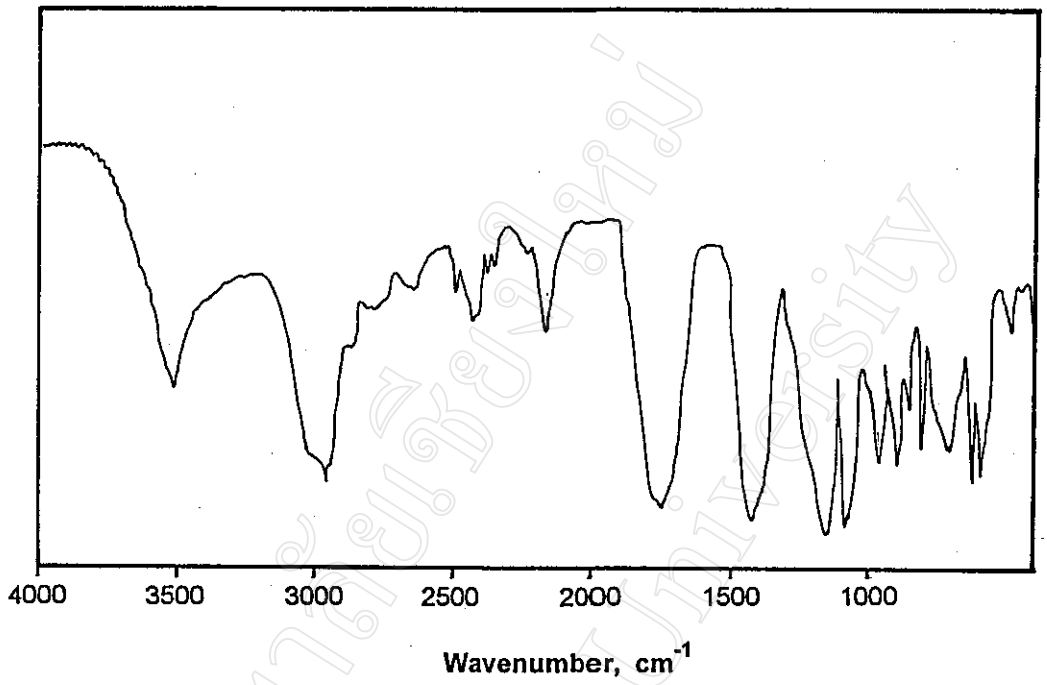

Fig. 3.23 : Infrared spectrum of purified poly(glycolic acid) synthesized at 150 °C for 24 hours using stannous octoate as initiator.

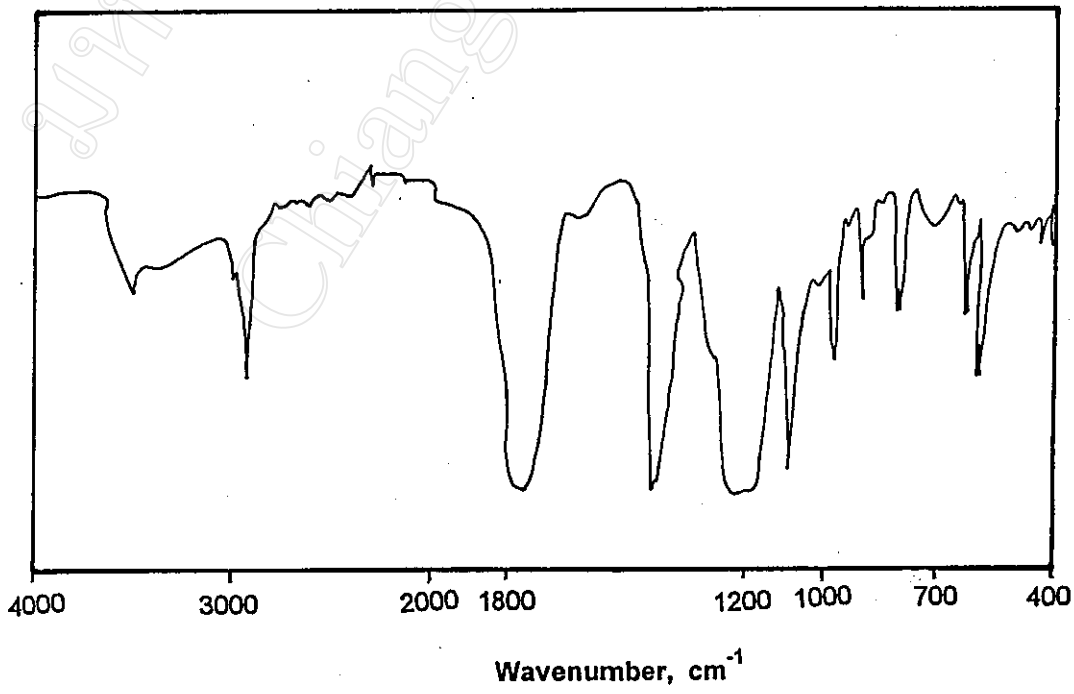

Fig 3.24 : Reference infrared spectrum of poly(glycolic acid) [121].

3.4.3.2 Temperature Transitions

A typical DSC curve for the purified PGA samples prepared in this work is illustrated in Fig. 3.25 showing the glass transition temperature (T_g) and crystalline melting point (T_m). The T_g (mid-point) and T_m (peak) values of 41.24°C (corrected to 41°C) and 219.62°C (corrected to 220°C) respectively are in close agreement with the corresponding literature values of 42°C [122] and 223°C [84].

In addition, the polymer's *heat of melting*, ΔH_m = 102.84 J/g, also printed out in Fig. 3.25, once again enables the % crystallinity to be calculated by comparison with the theoretical heat of melting for a 100% crystalline sample, ΔH_m^* = 206.75 J/g [84]. Thus,

$$\% \text{ crystallinity} = \frac{102.84 \text{ J/g}}{206.75 \text{ J/g}} \times 100\%$$

$$= 49.7\%$$

This % crystallinity reflects the relative ease with which the PGA chains, with their simple repeat units, can pack together in the crystal. At the same time, the polymer's exceptionally high T_m of 220°C, much higher than the previous polylactones (< 70°C), is generally attributed to its much lower ΔS_m in the governing thermodynamic equation :

$$T_m = \frac{\Delta H_m}{\Delta S_m}$$

where ΔS_m is the corresponding *entropy of melting*. This much lower ΔS_m is, in turn, generally attributed to the dipolar interactions between the PGA chains in the crystal being extensively reformed in the melt.

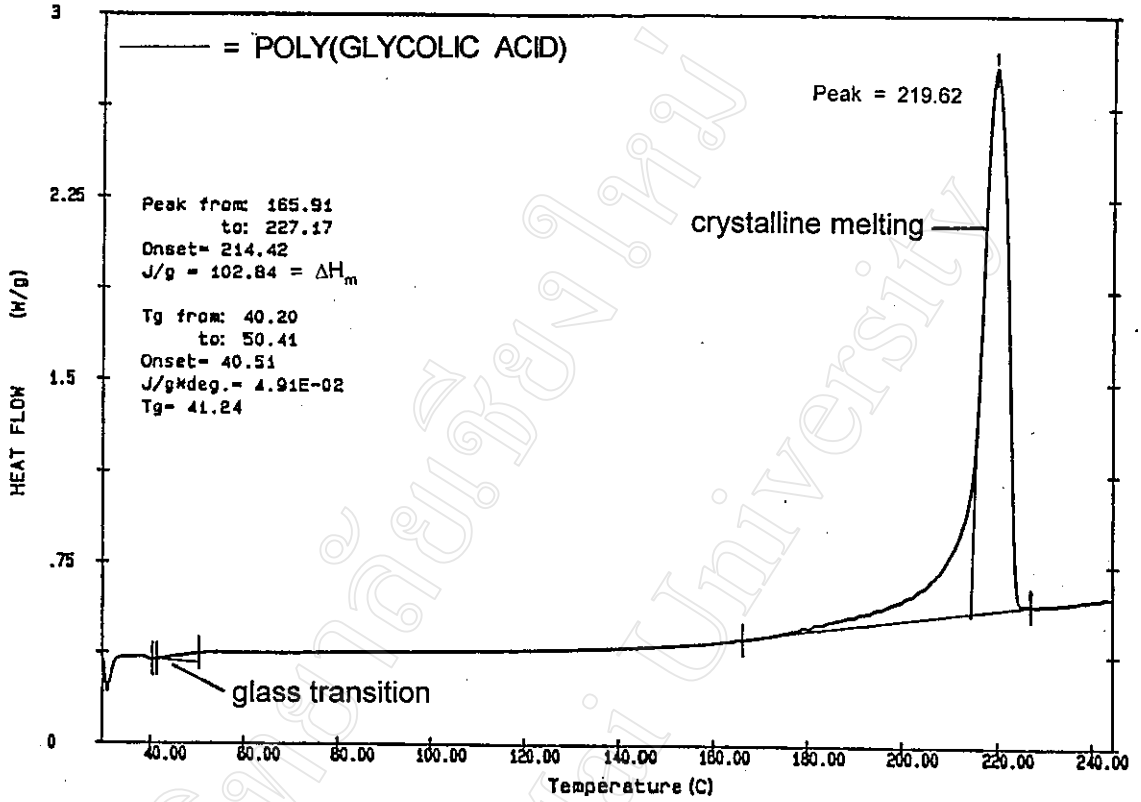

Fig. 3.25 : DSC thermogram of purified poly(glycolic acid) synthesized at 150°C for 24 hours using stannous octoate as initiator.

(Heating rate = 10°C/min; atmosphere = dry N_2)

3.4.3.3 Thermal Stability

A typical TG curve for the PGA synthesized here is shown in Fig. 3.26. The curve shows an essentially complete (≈ 98%) single-step weight loss over the temperature range 240-400°C. The close proximity of this decomposition range to the polymer's melting range determines that PGA has a very narrow "*processing window*" which is only about 10°C wide, i.e., around 230-240°C. Technologically, this attaches great importance to the need for precise temperature control during the melt processing of PGA, such as in suture production, if accompanying thermal degradation is to be avoided.

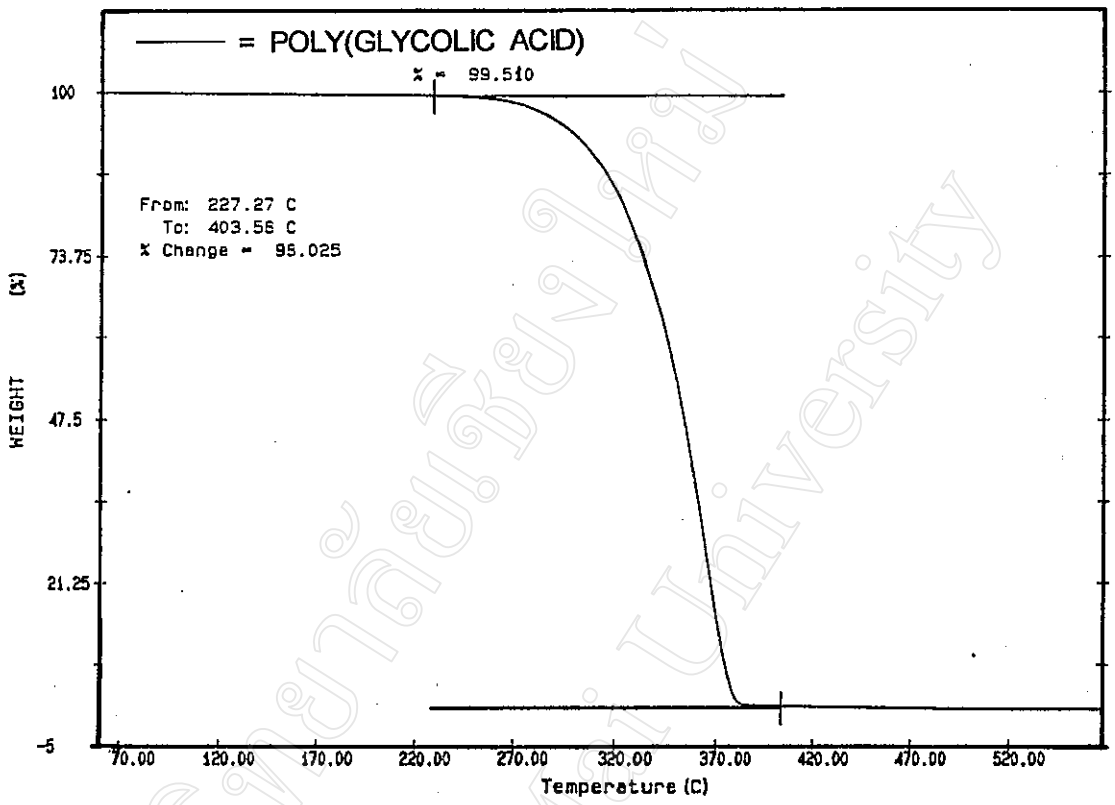

Fig. 3.26 : TG thermogram of purified poly(glycolic acid) synthesized at 150°C for 24 hours using stannous octoate as initiator.

(Heating rate = 20°C/min; atmosphere = dry N_2)

3.4.3.4 Molecular Weight

Because of its insolubility in all common organic solvents, molecular weight determination of the PGA products was not undertaken. Of the few solvents that are available, dimethylsulphoxide, benzyl alcohol and hexafluoroisopropanol are all potentially reactive (e.g., via hydrolysis/alcoholysis) with the polymer which introduces an element of uncertainty into molecular weight results. Commercial PGA sutures are usually reported as having number-average molecular weights, $\bar{M}_n$, in the region of 20,000-50,000 when polymerised at temperatures of around 200°C, the purity of the glycolide monomer being of critical importance.

3.5 L-Lactide

3.5.1 Polymerisation Procedure

In common with glycolide previously, L-lactide has also been widely studied since its polymer, poly(L-lactic acid) (PLLA), also finds extensive use in biomedical applications where biodegradability is required. L-lactide is similarly hygroscopic in contact with air, reverting easily to the parent L-lactic acid from which it is prepared. It should also be mentioned here that L-Lactide was chosen for this study in preference to its enantiomer, D-lactide, and its racemate, DL-lactide, for the following reasons:

(a) Studying a pure enantiomer eliminates from consideration any complicating effects which racemization may have on the results.

(b) Of the two enantiomer-specific polymers, poly(L-lactic acid), rather than the D-form, is the one which finds use in biomedical applications. This is because its hydrolysis product, L-lactic acid, is more readily metabolizable through the Krebs cycle than D-lactic acid.

(c) Being stereoregular, poly(L-lactic acid) is crystallisable with a characteristic melting point, useful to compare with the other polymers. Poly(DL-lactic acid), on the other hand, is completely amorphous.

For L-lactide, the series of polymerisation experiments that were carried out in this work are summarized in Table 3.44. The polymerisation procedure was exactly the same as that described in the previous section 3.4.1 (page 163) for glycolide except that the polymerisate was dissolved in chloroform as solvent and the polymer precipitated from solution by dropwise addition into ice-cooled absolute ethanol, an appropriate non-solvent, as shown in Fig. 3.2 (page 118). Unlike PGA, PLLA is easily soluble in a wide range of organic solvents.

3.5.2 Polymerisation Results

From the polymerisation profiles in Fig. 3.27, the initiator efficiency at each of the 3 temperatures studied was in the order of:

$$\text{Li}(t\text{-OBu}) \quad < \quad BF_3{\cdot}Et_2O \quad < \quad Sn(Oct)_2$$

Thus, the order of $BF_3{\cdot}Et_2O$ and $Sn(Oct)_2$ is reversed compared with all the previous cases. Indeed, the efficiency of the $Sn(Oct)_2$ initiator is so much greater than the others, especially at the two higher temperatures of 150°C and 180°C, that it tends to suggest that a substituted, and therefore sterically-hindered, monomer such as L-lactide may favour the monomer-insertion mechanism over the conventional ionic mechanisms. Its much lower rate at 100°C was again partly due to solidification of the polymerisate as the polymer's increasing melting point exceeded the reaction temperature. Other notable features in Fig. 3.27 include:

(1) At the highest temperature of 180°C, the $Sn(Oct)_2$-initiated reaction shows a decrease in % conversion at long reaction times, evidence of some thermal degradation having occurred.

(2) In the case of the $BF_3{\cdot}Et_2O$ and Li(*t*-OBu)-initiated reactions, the recorded 0% yields can be slightly misleading. In fact, this does not necessarily mean that no reaction occurred but rather that no recoverable solid polymer was obtained from the purification procedure. Indeed, the Li(*t*-OBu)-reactions at 150°C and 180°C yielded final products which resembled gels at room temperature. Obviously, some reaction had occurred but the products were of such low molecular weight that they could not be separated out as solid polymers.

(c) Surprisingly, the Li(*t*-OBu)-initiated reaction did produce solid polymer at the lowest temperature of 100°C. This could have been because transesterification was not yet competitive at this temperature, aided by the fact that the reaction was conducted mainly in the solid state. L-lactide, with its melting point of 95°C (cf., PLLA m. pt. 170-180°C), rapidly solidifies at 100°C as the polymerisation commences.

Table 3.44 : Summary of L-lactide polymerisation experiments.

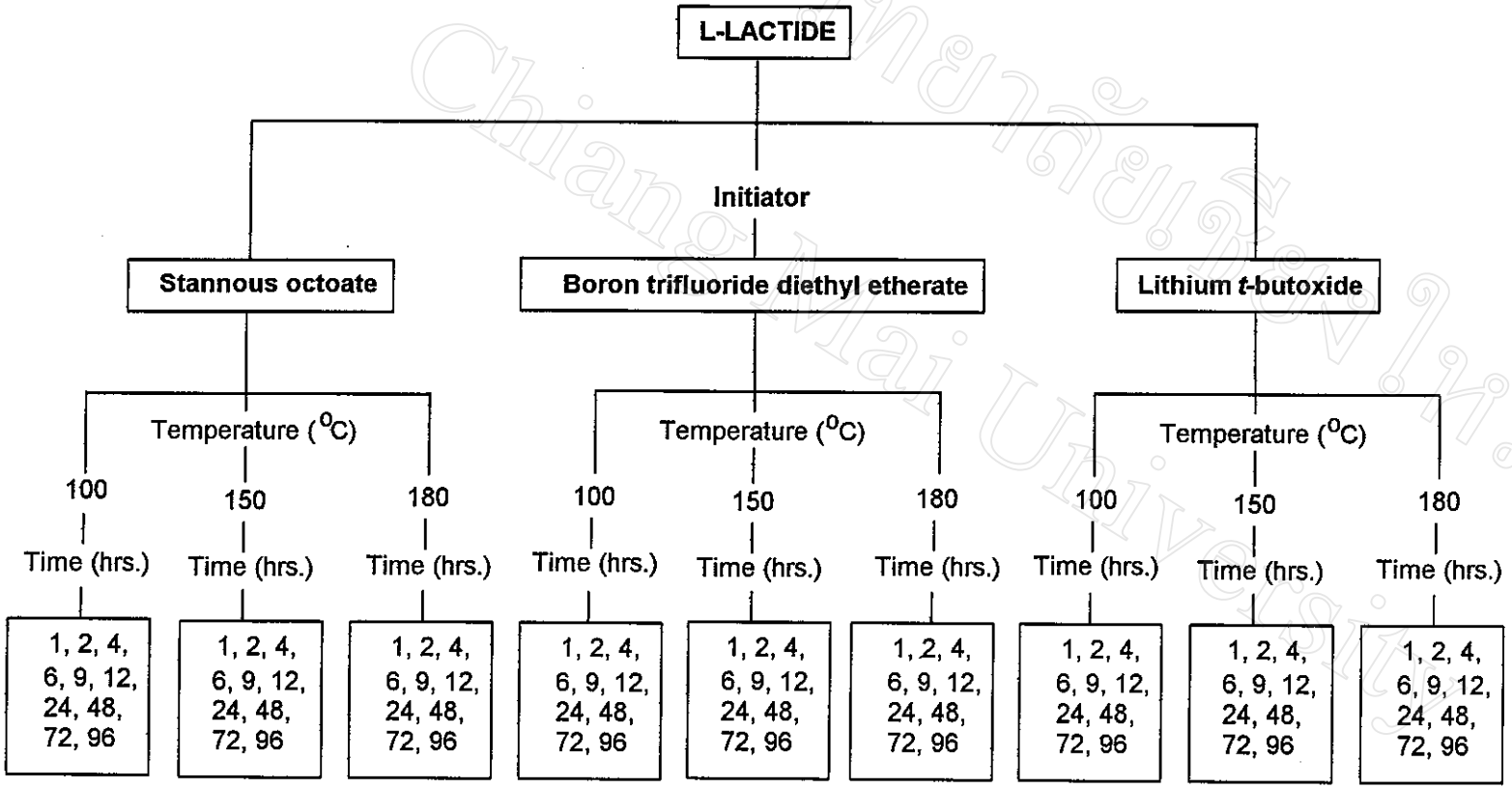

Table 3.45 : Polymerisations of L-lactide at 100°C using stannous octoate as initiator.

Monomer (g)	Initiator (g)	Time (hrs.)	Physical Appearance of Product at Room Temp.		Conversion (%)
			Crude	Purified	
1.428	0.0040	1	white solid	no solid ppte.	0
1.426	0.0040	2	white solid	white powder	5.8
1.422	0.0040	4	white solid	white powder	25.8
1.426	0.0040	6	white solid	white powder	36.1
1.422	0.0041	9	white solid	white powder	41.0
1.422	0.0040	12	white solid	white powder	46.8
1.420	0.0041	24	white solid	white powder	69.1
1.436	0.0041	48	white solid	white powder	89.4
1.419	0.0040	72	white solid	white powder	93.6
1.426	0.0040	96	white solid	white powder	93.9

Table 3.46 : Polymerisations of L-lactide at 150°C using stannous octoate as initiator.

Monomer (g)	Initiator (g)	Time (hrs.)	Physical Appearance of Product at Room Temp.		Conversion (%)
			Crude	Purified	
1.419	0.0039	1	white solid	white powder	82.9
1.425	0.0041	2	white solid	white powder	92.3
1.418	0.0040	4	white solid	white powder	90.1
1.429	0.0041	6	white solid	white powder	90.0
1.420	0.0039	9	white solid	white powder	91.7
1.417	0.0041	12	white solid	white powder	91.2
1.427	0.0040	24	white solid	white powder	89.4
1.420	0.0040	48	white solid	white powder	91.2
1.423	0.0039	72	white solid	white powder	89.0
1.431	0.0041	96	white solid	white powder	89.6

Table 3.47 : Polymerisations of L-lactide at 180°C using stannous octoate as initiator.

Monomer (g)	Initiator (g)	Time (hrs.)	Physical Appearance of Product at Room Temp.		Conversion (%)
			Crude	Purified	
1.423	0.0040	1	white solid	white powder	91.3
1.419	0.0040	2	white solid	white powder	91.6
1.426	0.0041	4	white solid	white powder	89.7
1.421	0.0039	6	white solid	white powder	86.7
1.422	0.0041	9	white solid	white powder	83.6
1.422	0.0041	12	white solid	white powder	83.2
1.424	0.0040	24	brown solid	brown powder	67.7
1.419	0.0040	48	brown solid	brown powder	69.8
1.422	0.0040	72	brown solid	brown powder	61.9
1.420	0.0040	96	brown solid	brown powder	72.2

Table 3.48 : Polymerisations of L-lactide at 100°C using boron trifluoride diethyl etherate as initiator.

Monomer (g)	Initiator (g)	Time (hrs.)	Physical Appearance of Product at Room Temp.		Conversion (%)
			Crude	Purified	
2.030	0.002	1	brown solid	no solid ppte.	0
2.028	0.002	2	brown solid	no solid ppte.	0
2.027	0.002	4	brown solid	no solid ppte.	0
2.026	0.002	6	brown solid	brown powder	4.4
2.030	0.002	9	brown solid	brown powder	13.0
2.028	0.002	12	brown solid	brown powder	17.9
2.034	0.002	24	brown solid	brown powder	55.4
3.119	0.003	48	brown solid	brown powder	49.5
2.034	0.002	72	brown solid	brown powder	58.0
2.029	0.002	96	brown solid	brown powder	94.1

Table 3.49 : Polymerisations of L-lactide at 150°C using boron trifluoride diethyl etherate as initiator.

Monomer (g)	Initiator (g)	Time (hrs.)	Physical Appearance of Product at Room Temp.		Conversion (%)
			Crude	Purified	
2.060	0.002	1	brown solid	no solid ppte.	0
2.035	0.002	2	brown solid	no solid ppte.	0
2.039	0.002	4	brown solid	no solid ppte.	0
2.050	0.002	6	brown solid	no solid ppte.	0
2.037	0.002	9	brown solid	no solid ppte.	0
2.034	0.002	12	brown solid	no solid ppte.	0
3.006	0.003	24	brown solid	brown powder	11.7
2.058	0.002	48	brown solid	brown powder	30.1
2.034	0.002	72	brown solid	brown powder	68.6
2.037	0.002	96	brown solid	brown powder	68.5

Table 3.50 : Polymerisations of L-lactide at 180°C using boron trifluoride diethyl etherate as initiator.

Monomer (g)	Initiator (g)	Time (hrs.)	Physical Appearance of Product at Room Temp.		Conversion (%)
			Crude	Purified	
2.031	0.002	1	brown solid	no solid ppte.	0
2.029	0.002	2	brown solid	no solid ppte.	0
2.043	0.002	4	brown solid	no solid ppte.	0
2.034	0.002	6	brown solid	no solid ppte.	0
2.023	0.002	9	brown solid	no solid ppte.	0
2.031	0.002	12	brown solid	brown powder	19.9
2.027	0.002	24	brown solid	brown powder	65.9
2.028	0.002	48	brown solid	brown powder	67.0
2.030	0.002	72	brown solid	brown powder	69.5
2.031	0.002	96	brown solid	brown powder	59.8

Table 3.51 : Polymerisations of L-lactide at 100°C using lithium *t*-butoxide as initiator.

Monomer (g)	Initiator (g)	Time (hrs.)	Physical Appearance of Product at Room Temp.		Conversion (%)
			Crude	Purified	
1.803	0.0010	1	brown solid	no solid ppte.	0
1.800	0.0010	2	brown solid	no solid ppte.	0
1.802	0.0010	4	brown solid	no solid ppte.	0
1.810	0.0011	6	brown solid	no solid ppte.	0
1.806	0.0010	9	brown solid	no solid ppte.	0
1.808	0.0011	12	brown solid	brown powder	12.3
1.802	0.0010	24	brown solid	brown powder	32.1
1.799	0.0010	48	brown solid	brown powder	36.9
1.820	0.0010	72	brown solid	brown powder	55.7
1.814	0.0011	96	brown solid	brown powder	77.8

Table 3.52 : Polymerisations of L-lactide at 150°C using lithium *t*-butoxide as initiator.

Monomer (g)	Initiator (g)	Time (hrs.)	Physical Appearance of Product at Room Temp.		Conversion (%)
			Crude	Purified	
1.824	0.0010	1	brown solid	no solid ppte.	0
1.814	0.0011	2	brown solid	no solid ppte.	0
1.820	0.0010	4	brown solid	no solid ppte.	0
1.825	0.0010	6	brown solid	no solid ppte.	0
1.823	0.0010	9	brown solid	no solid ppte.	0
1.826	0.0011	12	brown solid	brown gel	0
1.814	0.0010	24	brown solid	brown gel	0
1.816	0.0011	48	brown solid	brown gel	0
1.820	0.0010	72	brown solid	brown gel	0
1.812	0.0011	96	brown solid	brown gel	0

Table 3.53 : Polymerisations of L-lactide at 180°C using lithium *t*-butoxide as initiator.

Monomer (g)	Initiator (g)	Time (hrs.)	Physical Appearance of Product at Room Temp.		Conversion (%)
			Crude	Purified	
1.820	0.0010	1	brown solid	brown gel	0
1.818	0.0011	2	brown solid	brown gel	0
1.816	0.0010	4	brown solid	brown gel	0
1.822	0.0010	6	brown solid	brown gel	0
1.825	0.0010	9	brown solid	brown gel	0
1.826	0.0011	12	brown solid	brown gel	0
1.801	0.0010	24	brown solid	brown gel	0
1.799	0.0011	48	brown solid	brown gel	0
1.807	0.0010	72	brown solid	brown gel	0
1.799	0.0010	96	brown solid	brown gel	0

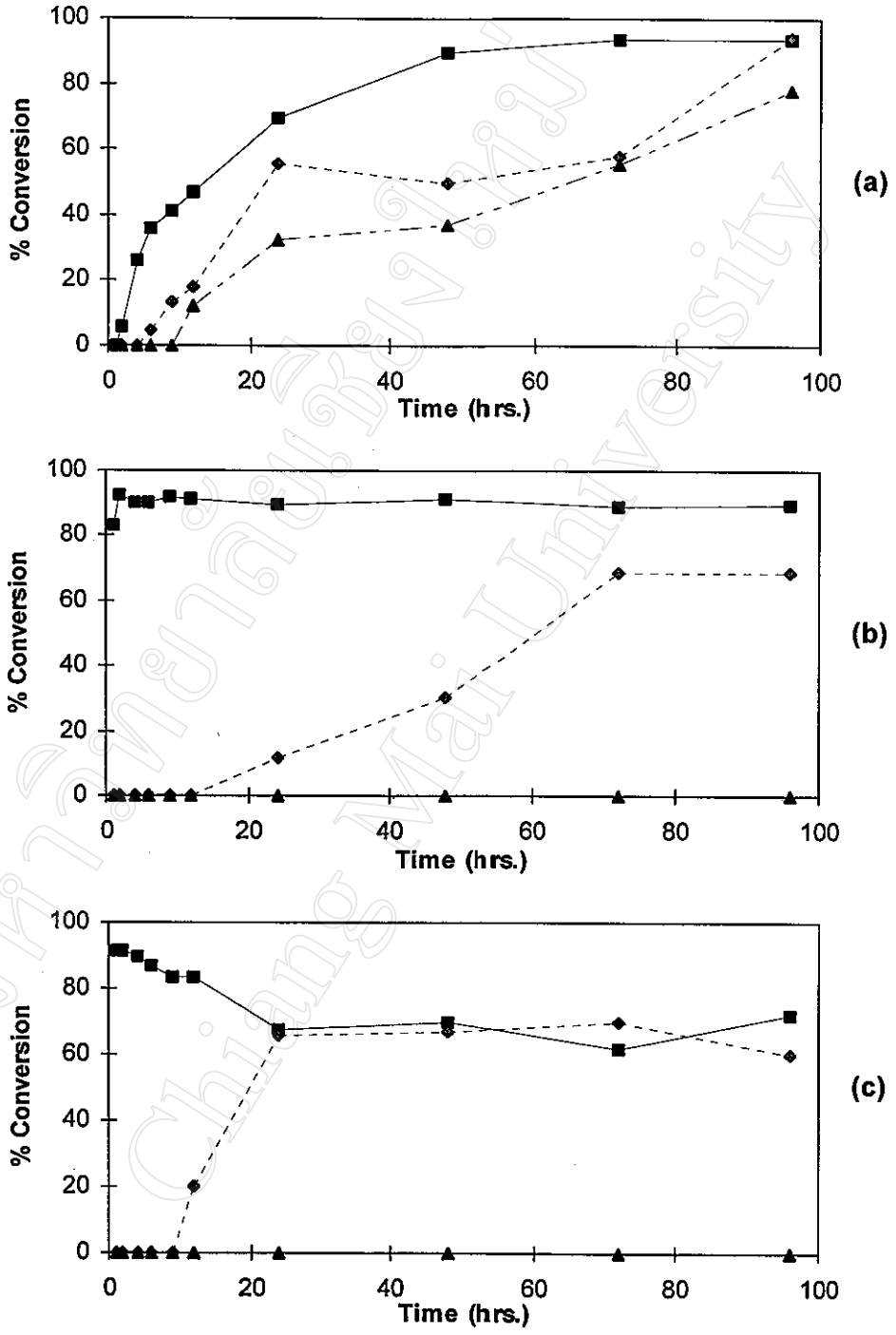

Fig. 3.27 : Comparison of L-lactide conversion-time profiles using different initiators at (a) 100°C (b) 150°C and (c) 180°C.

—■— $Sn(Oct)_2$
- -◆- - $BF_3{\cdot}Et_2O$
—▲- - Li(*t*-OBu)

3.5.3 Polymer Characterisation

3.5.3.1 Chemical Structure

A typical infrared spectrum of one of the purified poly(L-lactic acid) (PLLA) products is shown in Fig. 3.28. The spectrum, which was obtained from a sample prepared in the form of a thin film cast from solution in chloroform, compares very closely with the reference spectrum in Fig. 3.29. The major vibrational peak assignments are listed in Table 3.54.

Table 3.54 : Infrared absorption band assignments for poly(L-lactic acid).

Vibrational Assignment	Band Intensity*	Wavenumber (cm^{-1})
O-H stretching, in OH / COOH end-groups	w	3600-3400
C-H stretching, in CH / CH_3	m	3000, 2950
C=O stretching	s	1750
C-H bending, in CH / CH_3	m	1450-1380
C-O stretching, acyl-oxygen	s	1280
C-O stretching, alkyl-oxygen	s	1090

* w = weak m = medium s = strong

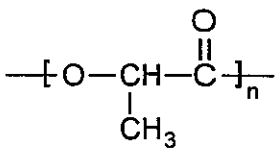

poly(L-lactic acid), PLLA

The PLLA spectrum in Fig 3.28 is therefore seen to be consistent with the polymer's chemical structure. The O-H stretching peak in the region of 3400-3600 cm^{-1}, due to the presence of residual OH and/or COOH end-groups in the polymer, is small for this particular sample and representative of its medium-range molecular weight (from GPC analysis : $\overline{M}_n$ = 11380, $\overline{DP}_n$ = 79).

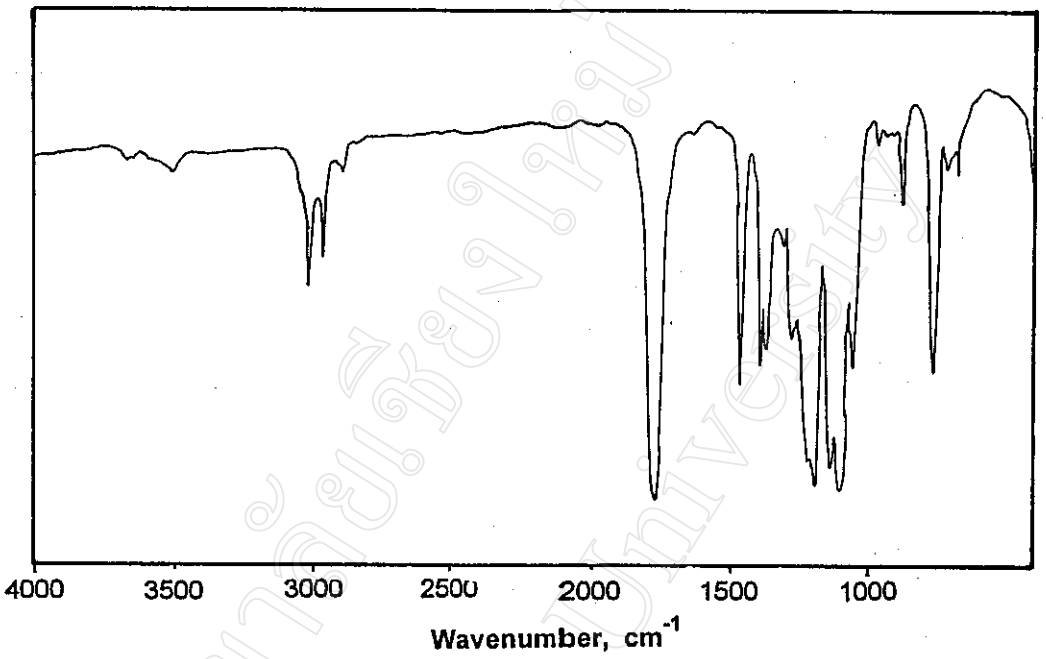

Fig. 3.28 : Infrared spectrum of purified poly(L-lactic acid) synthesized at 150°C for 24 hours using stannous octoate as initiator.

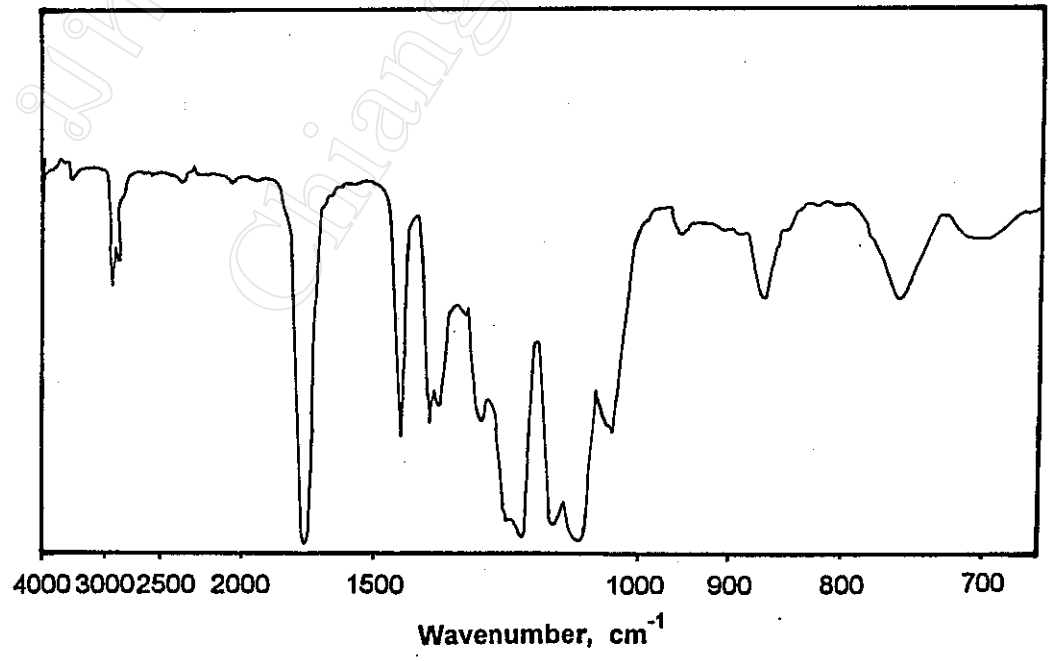

Fig 3.29 : Reference infrared spectrum of poly(L-lactic acid) [123].

3.5.3.2 Temperature Transitions

A typical DSC curve for the purified PLLA samples prepared in this work is illustrated in Fig. 3.30 showing the polymer's glass transition temperature (T_g) and crystalline melting point (T_m). The T_g (mid-point) and T_m (peak) values of 64.81°C (corrected to 65°C) and 176.27°C (corrected to 176°C) respectively are in close agreement with the corresponding literature values of 67°C and 172-174°C[122].

Additionally, from its heat of melting, ΔH_m = 46.73 J/g, also printed out in Fig. 3.26, the polymer's % crystallinity can be calculated from the equation:

$$\% \text{ crystallinity} = \frac{\Delta H_m}{\Delta H_m^* \text{ [84]}} \times 100\ \%$$

$$\% \text{ crystallinity} = \frac{46.73\ J/g}{92.84\ J/g} \times 100\%$$

$$= 50.3\ \%$$

When we compare PLLA's transition temperatures with those of PGA previously, it is interesting to note that the steric contribution of the CH_3 group in PLLA has opposite effects on T_g and T_m. Whereas it increases T_g (41°C → 65°C) as would be expected, it decreases T_m (220°C → 176°C). This implies that the CH_3 group's effect of increasing the energy barrier to chain rotation in the amorphous regions is not duplicated in the crystal. Of course, it is not necessary that it should be, since the glass transition and crystalline melting are fundamentally quite different in nature. However, it is usually the case in such structurally similar polymers that T_g and T_m follow the same trend. The fact that PLLA and PGA do not is probably the result of their different chain conformations in the crystal. PGA has a planar zig-zag chain conformation [125] whereas PLLA has a helical conformation [126]. Another possibility is the partial loss of stereoregularity in PLLA during its

synthesis caused by transesterification in the melt [145]. This would lead to partial racemization, crystal defects and a consequent lowering of ΔH_m and, therefore, T_m.

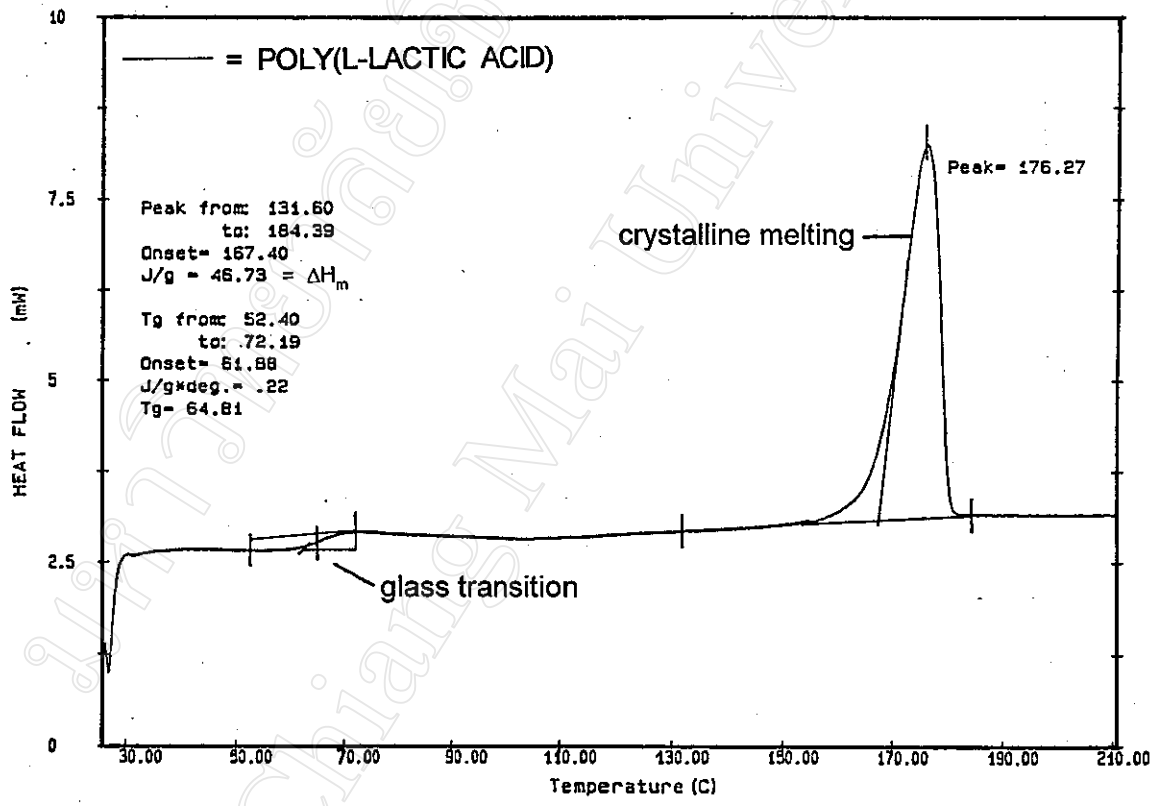

Fig. 3.30 : DSC thermogram of purified poly(L-lactic acid) synthesized at 150°C for 24 hours using stannous octoate as initiator.

(Heating rate = 10°C/min; atmosphere = dry N_2)

3.5.3.3 Thermal Stability

A typical TG curve for the PLLA synthesized here is shown in Fig. 3.31. The curve shows an essentially quantitative, single-step weight loss over the temperature range of 210-320°C. The small (approx. 0.6%) initial weight loss is probably due to moisture contamination.

When considered together with the previous DSC curve, PLLA is seen to have a slightly wider melt *processing window* (180-200°C) than PGA (230-240°C) previously. This is entirely due to its lower melting range.

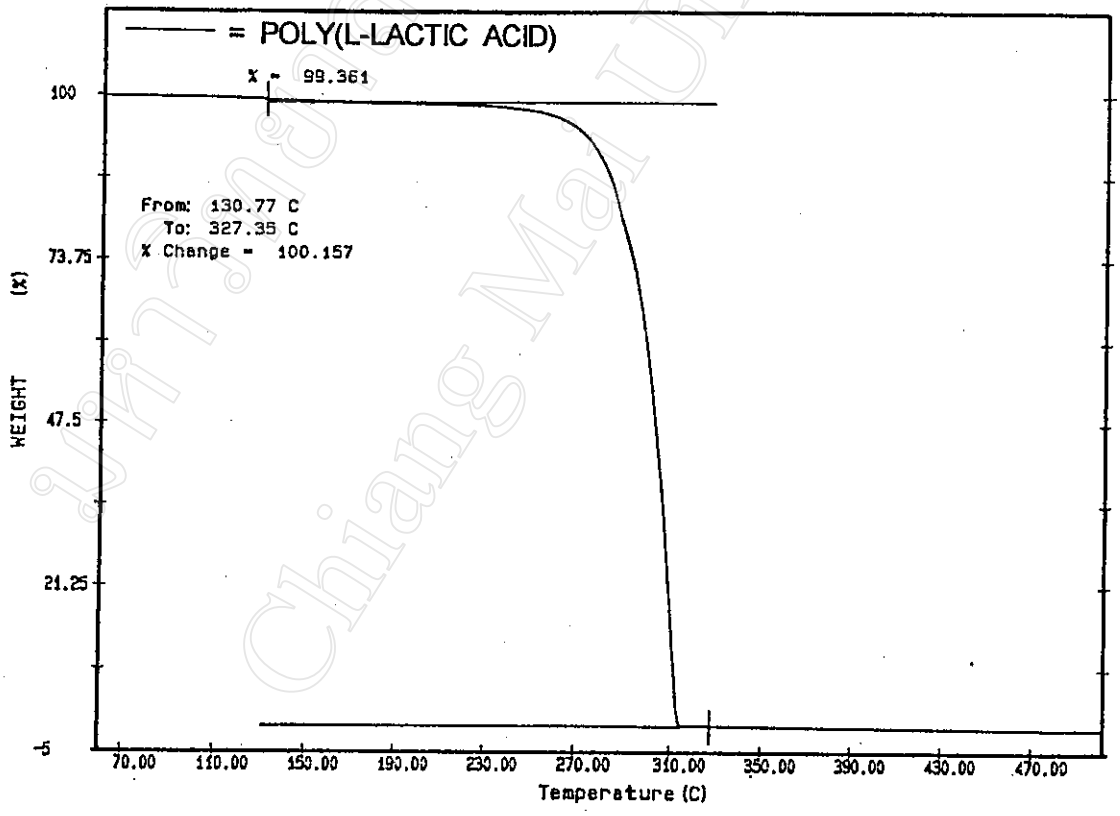

Fig. 3.31 : TG thermogram of purified poly(L-lactic acid) synthesized at 150°C for 24 hours using stannous octoate as initiator.

(Heating rate = 20°C/min; atmosphere = dry N_2)

3.5.3.4 Molecular Weight

For PLLA, the method of molecular weight determination used was gel permeation chromatography (GPC). GPC measurements were performed in chloroform ($CHCl_3$) as solvent at 30°C in a column calibrated by narrow molecular weight distribution polystyrene standards. Typical GPC curves and their associated data print-out are shown in Fig. 3.32. The results are summarized in Tables 3.55-3.61 for each of the 3 initiators used at each of the 3 polymerisation temperatures. For ease of comparison, the $\bar{M}_n$-time profiles are plotted in Fig. 3.33 from which the following general comments can be made:

(a) $Sn(Oct)_2$ consistently gave the highest molecular weights in the region of $\bar{M}_n$ = 10,000-15,000. This lends further weight to the earlier suggestion that ring substitution, as in L-lactide, may render the monomer more amenable to the monomer insertion-type polymerisation mechanism.

(b) At the highest temperature of 180°C, the molecular weight of the $Sn(Oct)_2$-initiated polymer decreases rapidly with time to a fairly constant level of $\bar{M}_n \approx$ 5,000. This confirms the earlier suspicion from the corresponding conversion-time profile that thermal degradation can occur at extended reaction times, especially as $Sn(Oct)_2$ is also known to be a transesterification catalyst.

(c) Apparently, no such degradation occurs at the lower temperature of 150°C which suggests that this might approach the optimum temperature for L-lactide polymerisation, combining a fast rate with high molecular weight.

(d) Even at the lowest temperature of 100°C, high molecular weight polymer can still be formed despite the fact that the reaction is conducted almost entirely in the solid-state.

TECHNICAL SERVICE, NATIONAL METAL AND MATERIALS TECHNOLOGY CENTER

Version 3.00a - MULTIDETECTOR GPC SOFTWARE - revised 03/17/93 J.Lesec

PLA/0.1%Sn(Oct)2/@150C/24hrs RESULTS Wed 03 SEP 1997 17:01:00
Polystyrene - 3 # 1 RUN # 22 Inj # 3 CODE : INJ 218
DATE : Wed 03 SEP 1997 TIME : 09:11:31 Manual integration
Calibration # 1.003 Number of points: 276 Axial dispersion: NO

MOLECULAR WEIGHTS		UNIVERSAL			
Peak mol. wt	Mp :	24390			
Number aver.	Mn :	11380			
Viscos. aver.	Mv :	25500			
Weight averag.	Mw :	32020			
Z average	Mz :	64280			
Polydispersity	:	2.81			
[n] (ml/g)	:	91.16			
Log(K) (M-H)	:	-.02406			
Alpha (M-H)	:	.45			
REFRACTOMETER C/c	: 1		Peak elution	: 15.651	Baseline : .10338
Area constant	: .6265		Conc. (g/ml)	: .00608	dn/dc : 0
VISCOMETER Mn	: 3772		Peak elution	: 15.34	Baseline : 1.0206
[n]area (ml/g)	: 93.59		[n]peak(ml/g)	: 106.5	[n]exp (ml/g) : 91.16

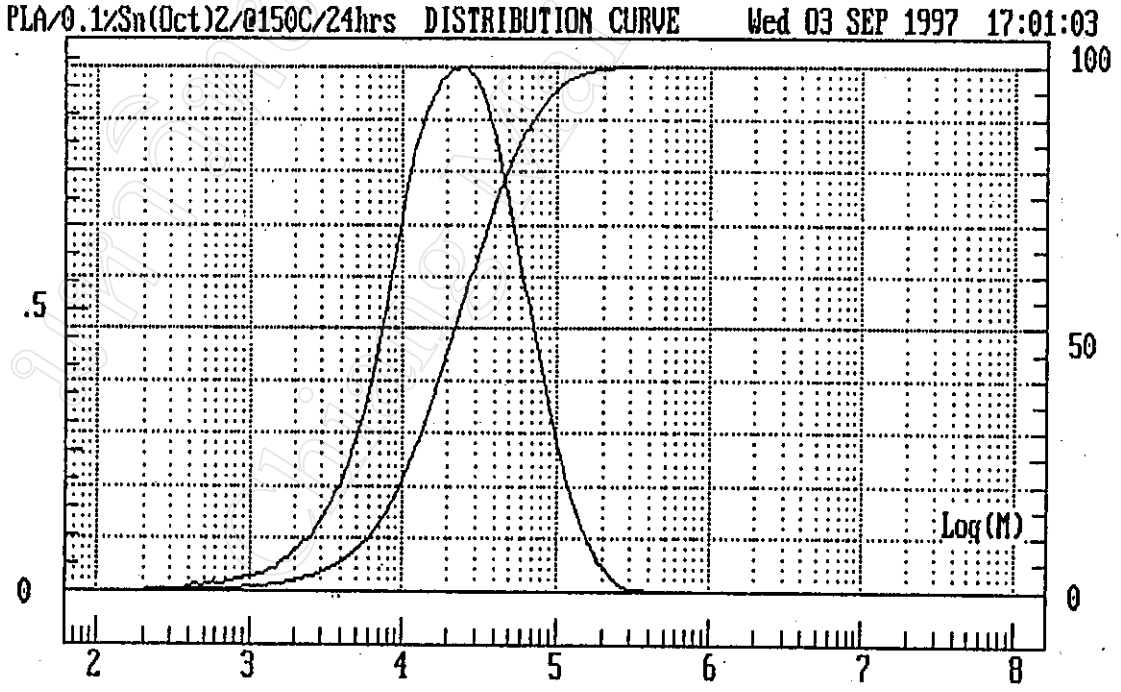

Fig. 3.32 : GPC curves and data print-out for purified poly(L-lactic acid) synthesized at 150°C for 24 hours using stannous octoate as initiator.

Table 3.55 : GPC molecular weight averages and polydispersity indices for the PLLA synthesized at 100°C using stannous octoate as initiator.

Polymerisation Time (hrs.)	Molecular Weight Averages			$\overline{M}_w / \overline{M}_n$
	$\overline{M}_n$	$\overline{M}_v$	$\overline{M}_w$	
4	12600	15270	17870	1.42
6	10950	14860	17540	1.60
9	13080	17350	21180	1.62
12	13190	16720	19930	1.51
24	14480	20740	24900	1.72
48	14360	22010	29250	2.04
72	13040	21470	26780	2.05
96	12250	20270	25400	2.07

Table 3.56 : GPC molecular weight averages and polydispersity indices for the PLLA synthesized at 150°C using stannous octoate as initiator.

Polymerisation Time (hrs.)	Molecular Weight Averages			$\overline{M}_w / \overline{M}_n$
	$\overline{M}_n$	$\overline{M}_v$	$\overline{M}_w$	
1	11290	33300	62070	5.50
2	11250	32100	56250	5.00
4	11200	35080	60590	5.41
6	12960	33600	51300	3.96
9	13570	35270	53790	3.96
12	14940	33500	47010	3.15
24	11380	25500	32020	2.81
48	12380	23210	27970	2.26
72	13230	25060	30600	2.31
96	11660	21970	26730	2.29

Table 3.57 : GPC molecular weight averages and polydispersity indices for the PLLA synthesized at 180°C using stannous octoate as initiator.

Polymerisation Time (hrs.)	Molecular Weight Averages			$\bar{M}_w / \bar{M}_n$
	$\bar{M}_n$	$\bar{M}_v$	$\bar{M}_w$	
1	14440	38490	57510	3.98
2	12770	35620	55670	4.36
4	13500	29720	39760	2.94
6	12960	25880	33170	2.56
9	10950	23990	30080	2.75
12	10140	18740	21960	2.17
24	5039	9290	10970	2.18
48	4693	8214	9983	2.13
72	4512	7338	8784	1.95
96	3351	5361	6545	1.95

Table 3.58 : GPC molecular weight averages and polydispersity indices for the PLLA synthesized at 100°C using boron trifluoride diethyl etherate as initiator.

Polymerisation Time (hrs.)	Molecular Weight Averages			$\bar{M}_w / \bar{M}_n$
	$\bar{M}_n$	$\bar{M}_v$	$\bar{M}_w$	
6	3085	3468	3648	1.18
9	3023	3576	3838	1.27
12	3103	3808	4377	1.41
24	5696	8171	8997	1.58
48	5824	8178	9056	1.55
72	4727	6396	6888	1.46
96	6670	9275	9442	1.42

Table 3.59 : GPC molecular weight averages and polydispersity indices for the PLLA synthesized at 150°C using boron trifluoride diethyl etherate as initiator.

Polymerisation Time (hrs.)	Molecular Weight Averages			$\bar{M}_w / \bar{M}_n$
	$\bar{M}_n$	$\bar{M}_v$	$\bar{M}_w$	
24	1730	1990	2018	1.17
48	2129	2486	2533	1.19
72	2706	3709	4038	1.49
96	2525	2694	2562	1.01

Table 3.60 : GPC molecular weight averages and polydispersity indices for the PLLA synthesized at 180°C using boron trifluoride diethyl etherate as initiator.

Polymerisation Time (hrs.)	Molecular Weight Averages			$\bar{M}_w / \bar{M}_n$
	$\bar{M}_n$	$\bar{M}_v$	$\bar{M}_w$	
12	1790	2040	2109	1.18
24	3478	4928	5625	1.62
48	4179	6764	7483	1.79
72	3497	5823	7159	2.05
96	2892	4559	6152	2.13

Table 3.61 : GPC molecular weight averages and polydispersity indices for the PLLA synthesized at 100°C using lithium *t*-butoxide as initiator.

Polymerisation Time (hrs.)	Molecular Weight Averages			$\overline{M}_w / \overline{M}_n$
	$\overline{M}_n$	$\overline{M}_v$	$\overline{M}_w$	
24	2394	2704	2798	1.17
48	4238	4985	5173	1.22
72	7242	9515	10600	1.46
96	9040	14590	17720	1.96

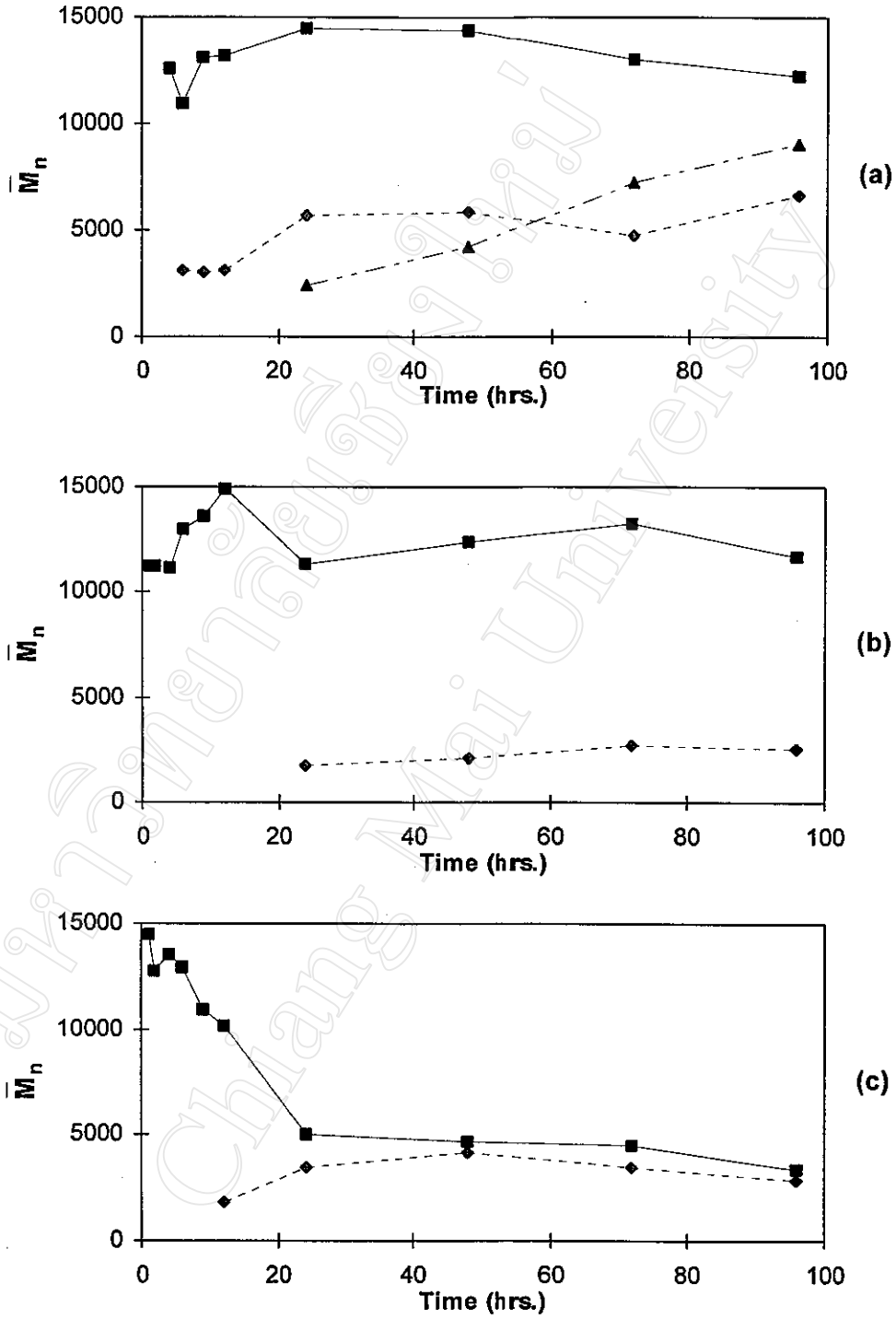

Fig. 3.33 : Comparison of PLLA number-average molecular weight $\bar{M}_n$-time profiles using different initiators at (a) 100°C (b) 150°C and (C) 180°C.

—■— $Sn(Oct)_2$
---◆--- BF_3·Et_2O
—▲— Li(*t*-OBu)

3.6 Tetramethyl Glycolide

3.6.1 Polymerisation Procedure

Tetramethyl glycolide is generally considered to be non-polymerisable, a common feature of tetrasubstituted glycolides. Nevertheless, it was included in this study in order to complete the series: glycolide, L-lactide, tetramethyl glycolide.

For tetramethyl glycolide, the series of polymerisation experiments that were carried out in this work are summarized in Table 3.62. The polymerisation procedure was the same as that described previously for glycolide and L-lactide except that only a single reaction temperature and time were chosen (150°C for 96 hours). At the end of the reaction, the polymerisate was dissolved in chloroform and the polymer (if any) precipitated from solution by dropwise addition into ice-cooled absolute ethanol.

3.6.2 Polymerisation Results

In each of the 3 polymerisations carried out, the only visibly discernable change which occurred during the timescale of the experiment was an increasing brown discoloration of the monomer. No discernable viscosity increase was observed and no polymer obtained.

Table 3.62 : Conditions used in the polymerisation of tetramethyl glycolide.

Monomer	Initiator		Temp.	Time	Physical Appearance of	Conversion
(g)	Type	Weight (g)	(°C)	(hrs.)	Final Product	(%)
0.855	$Sn(Oct)_2$	0.0021	150	96	no solid ppte.	0
0.989	$BF_3{\cdot}Et_2O$	0.001	150	96	no solid ppte.	0
1.078	Li(*t*-OBu)	0.0005	150	96	no solid ppte.	0

3.7 Main Conclusions

In this chapter, the ring-opening polymerisations of a series of 6 cyclic esters have been studied under identical reaction conditions which have allowed their reactivities to be compared. In order to relate their reactivities to their chemical structures, the 6 monomers have been divided into 2 series. The main conclusions to be drawn from the results presented in this chapter, and which will be expanded upon in subsequent chapters, are as follows:

SERIES I : Effect of Ring Size in Unsubstituted Lactones

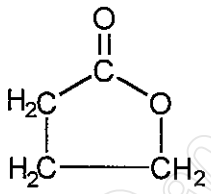

γ-butyrolactone

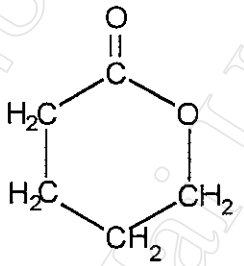

δ-valerolactone

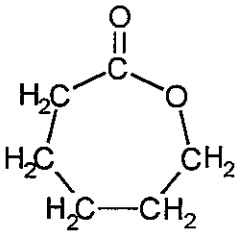

ε-caprolactone

1. Lactone polymerisability varies over the ring size range 5-7 as:

	γ-butyrolactone	<<	δ-valerolactone	>	ε-caprolactone
Ring size :	5		6		7

The 5-membered ring γ-butyrolactone is, to all intents and purposes, non-polymerisable due to its minimal ring strain. In contrast, the 6-membered ring δ-valerolactone is readily polymerisable but appears to approach its ceiling temperature above about 150°C. The 7-membered ring ε-caprolactone has a slightly lower polymerisability than δ-valerolactone in terms of rate but its polymer is thermally much more stable.

2. For each monomer, the order of the initiator efficiency, both in terms of rate and molecular weight build-up, is:

Initiator :	Li(*t*-OBu)	<	$Sn(Oct)_2$	<	$BF_3{\cdot}Et_2O$
Type :	anionic		monomer insertion		cationic

3. As would be expected, polymerisation rate increases markedly as the temperature is increased from 100°C to 150°C. However, there is evidence to suggest that at higher temperatures approaching 200°C, thermal decomposition of the polymer becomes increasingly competitive.

SERIES II : Effect of Substitution in 6-Membered Ring Glycolides

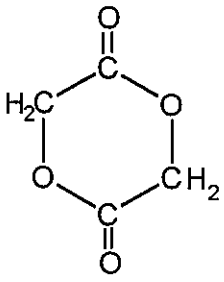

glycolide

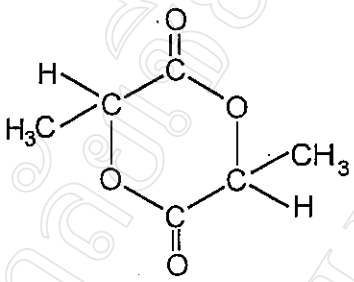

L-lactide

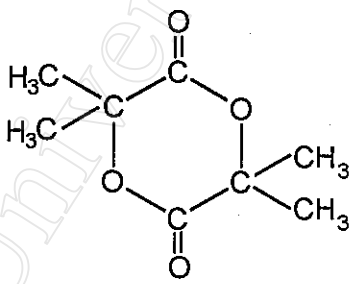

tetramethyl glycolide

1. Glycolide polymerisability decreases with ring substitution in the order:

   glycolide > L-lactide >> tetramethyl glycolide

   to the extent that tetramethyl glycolide is essentially non-polymerisable.

2. When compared with δ-valerolactone, its 6-membered ring lactone analogue, glycolide polymerises much faster at 150°C, i.e. at a temperature at which their melt-state polymerisations can be compared. At the lower temperature of 100°C, it is difficult to compare the two since poly(glycolic acid), PGA, solidifies very quickly at this temperature.

3. For glycolide, the order of initiator efficiency varies with temperature from:

   Li(*t*-OBu) < $Sn(Oct)_2$ < $BF_3{\cdot}Et_2O$ at 100°C

   to Li(*t*-OBu) ≈ $BF_3{\cdot}Et_2O$ < $Sn(Oct)_2$ at 150°C

For L-lactide, this order changes to:

Li(*t*-OBu) < $BF_3{\cdot}Et_2O$ < $Sn(Oct)_2$ at both temperatures

Comparisons at the highest temperature of 180°C are uncertain due to suspected loss by volatilisation of the $BF_3{\cdot}Et_2O$ initiator.

4. The expected increase in polymerisation rate with temperature is also a consequence of the longer time that the system can remain in the melt state before solidification occurs. This increase continues until the polymer starts to become thermally unstable.